Computers and Chemical Engineering 58 (2013) 116–134

Contents lists available at ScienceDirect

Computers and Chemical Engineering

journal homepage: www.elsevier.com/locate/compchemeng

Generalized shape constrained spline fitting for qualitative analysis of trends

Kris Villez[a,b,*], Venkat Venkatasubramanian[a,c], Raghunathan Rengaswamy[d]

[a] Laboratory for Intelligent Process Systems, School of Chemical Engineering, Purdue University, United States
[b] Spike, Department of Process Engineering, Eawag, Switzerland
[c] Department of Chemical Engineering, Columbia University, United States
[d] Department of Chemical Engineering, Indian Institute of Technology Madras, India

ARTICLE INFO

Article history:
Received 27 August 2012
Received in revised form 27 May 2013
Accepted 11 June 2013
Available online 4 July 2013

Keywords:
Data mining
Fault diagnosis
Qualitative trend analysis
Spline functions
Global optimization
Second order cone programming

ABSTRACT

In this work, we present a generalized method for analysis of data series based on shape constraint spline fitting which constitutes the first step toward a statistically optimal method for qualitative analysis of trends. The presented method is based on a branch-and-bound (B&B) algorithm which is applied for globally optimal fitting of a spline function subject to shape constraints. More specifically, the B&B algorithm searches for optimal argument values in which the sign of the fitted function and/or one or more of its derivatives change. We derive upper and lower bounding procedures for the B&B algorithm to efficiently converge to the global optimum. These bounds are based on existing solutions for shape constraint spline estimation via Second Order Cone Programs (SOCPs). The presented method is demonstrated with three different examples which are indicative of both the strengths and weaknesses of this method.

1. Introduction

This study was initiated in the context of qualitative analysis of trends. Such analysis concerns the abstraction of univariate or multivariate data series into qualitative descriptions. Most typically, qualitative analysis is focused on assessment of the sign of the first and/or second derivative of a time series. To do so, a data series is segmented into contiguous episodes within which the trends underlying to a data series are determined to have the same sign of the first derivative and/or second derivative. Such a segmentation is referred to as a qualitative representation (QR). We stress here that qualitative analysis of trends does not deal with the analysis of qualitative data which constitutes a particular branch in statistics of its own (Bryman & Burgess, 1993; Miles & Huberman, 1994). In what follows, we will use the term qualitative analysis for qualitative analysis of data series.

So far, qualitative analysis has primarily gained attention in the engineering literature. In this context, qualitative analysis enables to tie coarse-grained expert knowledge with automated, on-line data-based assessment tools. Typical engineering challenges attacked with this approach are process data mining (Stephanopoulos, Locher, Duff, Kamimura, & Stephanopoulos, 1997; Villez et al., 2007), reaction end-point detection (Villez, Rosén, Anctil, Duchesne, & Vanrolleghem, 2008, 2012) and, most popularly, process fault detection and identification (FDI) (Colomer, Melendez, & Gamero, 2002; Janusz & Venkatasubramanian, 1991; Maurya, Paritosh, Rengaswamy, & Venkatasubramanian, 2010; Maurya, Rengaswamy, & Venkatasubramanian, 2005; Rengaswamy & Venkatasubramanian, 1995; Rubio, Ruiz, & Mélendez, 2004; Venkatasubramanian, Rengaswamy, & Kavuri, 2003; Villez, Keser, & Rieger, 2009). The main advantage lies in the limited requirements for detailed process models or control design. Indeed, intuitive rule bases or tables can easily be generated and used to determine proper action once a QR of a time series is obtained (e.g., Villez et al., 2008).

A common characteristic of the existing methods for qualitative analysis is an extensive use of heuristics and/or tuning parameters and the absence of a well-defined global objective. For instance, the wavelet-based method developed in Bakshi and Stephanopoulos (1994) relies on a heuristic proposed by Witkin (1983) which determines the QR. The methods in Dash, Maurya, Venkatasubramanian, and Rengaswamy (2004) and Charbonnier, Garcia-Beltan, Cadet, and Gentil (2005) are based on piece-wise polynomial fitting. They make use of recursive schemes for on-line updating of the set of piece-wise polynomials. Because the optimal specification of interval endpoints for the piece-wise polynomials is NP-hard, locally optimal strategies based on lack-of-fit statistics are used.

* Corresponding author at: Spike, Department of Process Engineering, Eawag, Switzerland. Tel.: +41 58 765 5280; fax: +41 58 765 5389.
E-mail address: kris.villez@eawag.ch (K. Villez).

0098-1354/$ – see front matter © 2013 Elsevier Ltd. All rights reserved.
http://dx.doi.org/10.1016/j.compchemeng.2013.06.005

List of acronyms and symbols

a, b	left/right interval endpoint (scalar)
a_i, b_i	interval endpoints or knot arguments (scalar)
c_{ij}, x_{ij}, y_{ij}	element of matrix $C/X/Y$ on row i, column j (scalar)
c_i, x_i, y_i	ith element of vector $\mathbf{c}/\mathbf{x}/\mathbf{y}$ (scalar)
$\mathbf{c}$, $\mathbf{x}$, $\mathbf{y}$	column vectors
e	index of episodes (integer)
$f(t)$	univariate function in t
$f^{(k)}(t)$	kth derivative with respect to t of function f
$\mathbf{g}_{q+j,k}$	vector of linear coefficients to project the spline basis coefficients, $\mathbf{c}$, onto the piece-wise polynomial basis coefficients of degree k in interval $q+j$
h, i, j, q, r	index variables (integer)
k	order of monomial or derivative (integer)
l_e, u_e	lower and upper limit for right episode endpoint (scalar)
m	number of interval endpoints or knots (integer)
n	degree of polynomial or spline function (integer)
n_e	number of episodes (integer)
p_k	polynomial coefficient of order k (scalar)
$s_{e,k}$	sign of derivative of order k in episode e (+1, 0, or −1)
t	function argument (scalar)
$t_{e,1}$	left episode endpoint (scalar)
t_e, $t_{e,2}$, t_s	right episode endpoint (scalar)
B&B	Branch and Bound
$\mathbf{C}$, $\mathbf{X}$, $\mathbf{Y}$	matrices
DP	Dynamic Program
$F(\mathbf{y}, \mathbf{c})$	objective function in $\mathbf{y}$ and $\mathbf{c}$, convex in $\mathbf{c}$
F_L	Lower bound
F_{OPT}	Global optimum objective function
F_R	Reduced upper bound
F_U	Upper bound
MAP	Maximum A posteriori Probability
NLP	Non-Linear Program
QR	Qualitative Representation
QS	Qualitative Sequence
SCS	Shape Constrained Spline
SCSDP1	Shape Constrained Spline Diagnosis Procedure 1
SCSDP2	Shape Constrained Spline Diagnosis Procedure 2
SDP	Semi-Definite Program
SOC	Second Order Cone
SOCP	Second Order Cone Program
SSR	Sum of Squared Residuals
$\mathcal{A}$, $\mathcal{D}$	Sets of argument values
$\mathcal{C}_L$, $\mathcal{C}_U$	Set of spline coefficients for the lower/upper bound
$\mathcal{T}$	Set of feasible endpoints
λ_k	Regularization parameter for derivative or order k
σ	Noise standard deviation

Furthermore, it is indicated in Villez (2007) that these methods optimize the piece-wise polynomial representation to derive the QR rather than optimizing the QR itself. The methods in Cao and Rhinehart (1995) and Flehmig, Watzdorf, and Marquardt (1998) are based on filters set up for the assessment of the sign of a single derivative only. Joint analysis of the signs for more than one derivative has not been considered in this case. Multivariate qualitative analysis of trends, i.e., in which a multivariate data series is analyzed jointly, has only been considered so far in Flehmig and Marquardt (2006). Note that all existing methods consider a single explanatory variable only, which is time in all of the reported applications. We conclude this overview by stressing that the development and application of suboptimal methods can be a valid choice for on-line applications on grounds of computational speed.

Our primary motivation for this study is to provide a provably global optimal method for qualitative analysis. To this end, the problem of qualitative analysis is formulated for the first time as a shape constrained function fitting problem. Shape Constrained Spline (SCS) fitting is a non-parametric estimation problem with so called order restrictions on the spline function value and/or its derivatives. Alternative non-parametric models include kernel regression models and are almost exclusively related to monotonicity constraints (Delecroix, Simioni, & Thomas-Agnan, 1996; Dette, Neumeyer, & Pilz, 2006; Dette & Pilz, 2006; Hall, Huang, Gifford, & Gijbels, 2001; Holmes & Heard, 2003; Lavine & Mockus, 1995; Leitenstorfer & Tutz, 2007; Mammen, 1991; Meyer & Habtzghi, 2011; Robertson, Wright, & Dykstra, 1988). An exception is provided in Habtzghi and Datta (2012) in which other simple shapes are also considered, namely convex, monotone convex, or concave-convex. In Delecroix and Thomas-Agnan (2000) and Mammen, Marron, Turlach, and Wand (2001) both spline- and kernel-based approaches are discussed jointly.

A large fraction of the literature on SCS fitting deals with finding the optimal fit of positive, monotone, or convex spline functions, where optimality is defined as a least-squares or regularized objective function (Beliakov, 2000; Brunk, 1955; Dierckx, 1980; Fritsch, 1990; He & Shi, 1998; Kelly & Rice, 1990; Mammen & Thomas-Agnan, 1999; Meyer, 2008; Mukerjee, 1988; Ramsay, 1988, 1998; Tantiyaswasdikul & Woodroofe, 1994; Utreras, 1985; Wang & Li, 2008; Wegman & Wright, 1983; Wright & Wegman, 1980). More complex monotonic convex and monotonic concave shapes are applied by Elfving and Andersson (1988). In Hazelton and Turlach (2011), any shape constraint can be applied as long as it can be expressed in the form of a finite number of linear inequalities in the spline coefficients. To make this possible, the order of the spline is typically constrained to be equal or lower than two (linear) or three (quadratic). In this case, the feasible set of spline functions can be represented by polyhedral cones. Specific algorithms for such problems are provided in Dykstra (1983), Fraser and Massam (1989) and Meyer (1999). Alternatively, it is possible to formulate overly constrained solutions to ensure shape satisfaction of higher order splines. An approximate solution for monotone cubic splines in Meyer (2008) is based on solving first with a set of necessary but insufficient constraints which lead to satisfaction of the shape constraints in the knots of the splines. A subsequent interpolation procedure is used to obtain a spline function which satisfies the shape constraints over the whole function domain. In Turlach (2005), a more general method is proposed for splines constrained to any sort of shape. It is based on a two-step procedure in which violated constraints are identified and then mitigated by adding linear inequality and equality constraints. Both approaches are suboptimal because the resulting spline function is overly constrained. In contrast, Wang and Li (2008) recognize that sufficient and necessary conditions for monotone cubic splines can be formulated as SOC constraints. The more general idea that shape constraints on polynomials of any order can be represented as Semi-Definiteness constraints is presented in Nesterov (2000). SOC constraints are special instances of Semi-Definiteness constraints which result when the shape constrained polynomial is of third or lower order. As a result, spline functions up to 4th (cubic), 5th (quartic), and 6th (quintic) order with positive, monotone, and convex shape constraints, respectively, can be fitted efficiently with Interior Point optimization algorithms (Papp, 2011).

A few studies provide methods for more complex shape constraints (Hazelton & Turlach, 2011; Papp, 2011; Turlach, 2005). However, the provided methods assume that the intervals over which shape constraints are applied are known in advance. As a

Table 1
Overview of primitives as function of the first and second derivative. In this table, the function value is considered unspecified.

Characters (signs)		Sign of first derivative							
		?		–		0		+	
Sign of second derivative	?	Q	(?,?)	L	(–,?)	–		H	(+,?)
	+	P	(?,+)	A	(–,+)	–		B	(+,+)
	0	O	(?,0)	E	(–,0)	F	(0,0)	G	(+,0)
	-	N	(?,–)	D	(–,–)	–		C	(+,–)

result it is impossible with these methods to optimally fit a function which is constrained to exhibit a complex shape such as convex-concave-convex while simultaneously estimating the arguments in the domain where the shape changes. This particular problem constitutes the focus of this manuscript.

Solving this problem is especially relevant in the context of qualitative analysis for Fault Detection and Identification applications. These are based on established relations between particular shapes and diagnostic results. In this paper, we refer to such a shape as a qualitative sequence (QS), i.e. an ordered list of elementary shapes (e.g., convex-concave-convex). It is typical that domain experts can match such QSs with diagnostic results based on past experiences or on first principles understanding of the monitored process. Similarly, one can represent particular scenarios obtained by Qualitative Simulation (QSIM, Kuipers, 1994) as a QS. Importantly, the argument values of the fitted function in which the shape changes, from here on referred to as transitions, are not specified a priori. To verify whether a particular QS corresponds well with a given time series, we develop a method in this paper by which the transition points are located optimally. This leads to the QR, which is a segmentation of a time series according to the applied shape constraints. The obtained QR corresponds to the best fit of a spline function conditional to a given QS. This is expected to be useful for process supervision as FDI problems can then be formulated as one of finding one or more QS for which the resulting lack-of-fit is low. It is noted that the current form of the provided method requires that one identifies all fault scenarios a priori and that one assigns an unique QS to each of the scenarios.

Qualitative analysis has so far been applied with a single explanatory variable only. As such, the focus in the above overview on univariate spline functions is natural. Nevertheless, it is noted that research on SCS functions in a multivariate context has largely been limited to simple constraints (positive, monotone, convex) (see e.g., Beliakov, 2000; Cai & Dunson, 2007; Friedman & Tibshirani, 1984; Villalobos & Wahba, 1987; Wang & Li, 2008).

The structure of the remainder of this paper is as follows. The developed method is presented in the next section (Section 2, Methods) after which exemplary results of its application are given in the Results section (Section 3). This is followed by a Discussion section (Section 4) in which the results are interpreted more deeply and remaining research questions are presented. Finally, with Conclusions (Section 5) we summarize the contents of this paper.

2. Method

The following pages present the existing and newly developed methods in this work. Definitions are provided first (Section 2.1). This is followed by the description of an existing method for shape constrained spline (SCS) fitting based on a Second Order Cone Program (SOCP) formulation (Section 2.2). In Section 2.3, the newly developed method for generalized SCS fitting based on a branch-and-bound (B&B) algorithm is presented. A list of symbols and abbreviations is added at the end of this article.

2.1. Definitions

In this section, we provide the required definitions for accurate description of the provided methods.

Primitive A primitive is defined as a unique set of qualitative values (positive (+), zero (0), negative (–), or unknown (?)) for a function value and its derivatives up to the second derivative. It is typical to associate an alphabetic character or symbol to each unique set. The unknown value (?) is taken from Kuipers (1994) and allows to formally express that a certain sign is left unspecified.

Episode An episode is defined as a non-empty interval of the argument of a function over which the function is characterized by a single primitive.

Qualitative Representation (QR) A QR of a time series is the description of a time series by means of contiguous, i.e., consecutive and non-overlapping, episodes.

Qualitative Sequence (QS) A QS of a time series is the description of a time series by means of consecutive primitives.

Primitives are used to describe univariate functions in terms of their shape in non-empty intervals. For instance, a positive (negative, zero) second derivative corresponds to a convex (concave, linear) shape. Similarly, a positive (negative, zero) first derivative corresponds to an isotonic (antitonic, flat) shape. Primitives are usually represented by means of a unique character for each combination of signs for the first and second derivative.

Table 1 shows the characters as used in this study for all possible values for the sign of the first and second derivatives. Seven unique characters are usually reported (e.g., Cheung & Stephanopoulos, 1990; Maurya et al., 2005; Villez et al., 2012) for the cases where both signs are known (A to G). These are referred to as triangular primitives (also: triangular components, Cheung & Stephanopoulos, 1990). In Janusz and Venkatasubramanian (1991) and Rengaswamy and Venkatasubramanian (1995), nine primitives are used by allowing a single change in the sign of the first derivative in two additional primitives.

Six additional characters are associated with primitives for which the sign of the first and/or second derivative is unknown (H, L, and N to Q). When only the first derivative is known (H, L), the primitive is referred to as a *monotonic primitive* (Villez et al., 2008, 2012). Likewise, we propose the term *monocurvature primitive* for those where the sign of the second derivative is only known

(N, O, P). Even though the characters can be assigned arbitrarily, they are assigned here so as to convey some meaning where possible. Specifically, this is so for characters A (antitonic acceleration), D (deceleration), F (flat), L (low), H (high), N (negative), O (zero), P (positive), and Q (question marks). In order to specify the sign of the function value we choose to use a superscript ($^+$, $^\circ$, $^-$, $^?$) to indicate the function value, e.g., A^+ for a positive, antitonic, convex shape. The unknown superscript ($^?$) is assumed if none is given, i.e., $A \equiv A^?$. A zero-valued first derivative over a non-empty interval automatically implies a zero-valued second derivative. Similarly, a zero-valued function implies a zero-valued first and second derivative. This means that the symbols H°, L°, N°, O°, P°, and Q° are automatically replaced by F° to ensure the uniqueness of the characters in use. As a result, F° is the only applicable primitive with the $^\circ$ as superscript.

A *qualitative representation* is obtained when an univariate function is segmented so that (1) a contiguous arrangement of segments results and (2) each segment is characterized by a single primitive and its bounds on the interval of the function arguments. Each resulting segment is referred to as an *episode*. Each episode is described uniquely by (1) a left- and right-side endpoint and (2) the signs of the function, first episode, and second derivatives. The endpoints shared by two consecutive episodes are also referred to as *transitions*. For n_e episodes there are thus $n_e + 1$ unique episode endpoints of which $n_e - 1$ are transitions. A complete QR with n_e episodes can be described formally as follows:

$$QR = \{(s_{1,0}, s_{1,1}, s_{1,2}, t_{1,1}, t_{1,2}), \ldots, (s_{e,0}, s_{e,1}, s_{e,2}, t_{e,1}, t_{e,2}), \ldots, (s_{n_e,0}, s_{n_e,1}, s_{n_e,2}, t_{n_e,1}, t_{n_e,2})\} \quad (1)$$

with

$$s_{e,0}, s_{e,1}, s_{e,2} \in \{?, -, 0, +\}$$

Since the episodes in a QR are contiguous, it holds that:

$$t_{e,2} = t_{e+1,1} \quad (2)$$

When the endpoints are unknown, the obtained description is referred to as a qualitative sequence (QS). In other words, a QS defines the sequence of primitives for an univariate function without specifying the corresponding episode endpoints. Formally, one writes:

$$QS = \{(s_{1,0}, s_{1,1}, s_{1,2}), \ldots, (s_{e,0}, s_{e,1}, s_{e,2}), \ldots, (s_{n_e,0}, s_{n_e,1}, s_{n_e,2})\} \quad (3)$$

As indicated in Section 1, it is assumed that one or more QSs are given and that one seeks to find a parametrized function which satisfies these QS while fitting a data series optimally. The next section (Section 2.2) explains how one can obtain an optimal function fit corresponding to a QR, i.e., with the endpoints specified. In the following section (Section 2.3) it is explained how the endpoints can be located optimally. This results in an optimal function fit conditional to a QS only, thus without specifying the endpoints a priori.

2.2. Identifying Shape Constrained Spline (SCS) functions with a given Qualitative Representation (QR)

Existing methods for Shape Constrained Spline (SCS) fitting aim at the optimal fit of a spline function which satisfies a given QR. In our opinion, the most general approach to date is reported in Papp (2011). We describe the original method first as well as some of the limitations, followed by solutions to these limitations. For a general introduction to spline function fitting and – more broadly – functional data analysis we refer to de Boor (1978) and Ramsay and Silverman (2005).

2.2.1. Original method

The first element of the method for SCS fitting is provided by Nesterov (2000) and describes the necessary and sufficient conditions for non-negativity of a polynomial of given degree over a given argument interval. These conditions can be written as follows: For a polynomial of degree $n = 2 \cdot m + 1, f(t) = \sum_{k=0\ldots n} p_k \cdot t^k$, $p_k, a, b \in \mathbb{R}$ and positive semi-definite (p.s.d.) symmetric matrices $\mathbf{X} = (x_{ij})_{i,j=0\ldots m}$ and $\mathbf{Y} = (y_{ij})_{i,j=0\ldots m}$, it holds that

$$f(t) \geq 0 | a < t < b \Leftrightarrow \exists X, Y | p_k = \sum_{i+j=k} (-a \cdot x_{ij} + b \cdot y_{ij}) + \sum_{i+j=k-1} (x_{ij} y_{ij}) \quad (4)$$

For a polynomial of degree $n = 2 \cdot m, f(t) = \sum_{k=0\ldots n} p_k \cdot t_k$, $p_k, a, b \in \mathbb{R}$, positive semi-definite (p.s.d.) symmetric matrices $X = (x_{ij})_{i,j=0\ldots m}$, and $Y = (y_{ij})_{i,j=0\ldots m}$ it holds that

$$f(t) \geq 0 | a < t < b \Leftrightarrow \exists X, Y | p_k = \sum_{i+j=k} (x_{ij} - a \cdot b \cdot y_{ij}) + \sum_{i+j=k-1} (a + b) \cdot y_{ij} - \sum_{i+j=k-2} y_{ij} \quad (5)$$

The above conditions express that the application of a non-negativity constraint to a polynomial of a given degree is equivalent to the search for two positive semi-definite symmetric matrices of which the elements are subject to linear equality constraints. Similar non-positivity constraints are obtained by multiplying the left-hand sides in Eqs. (4) and (5) with -1 (i.e., so they read as: $f(t) \leq 0 \ldots - p_k \ldots$). This leads to a semi-definite program (SDP) which is hard to solve in the general case (Alizadeh & Goldfarb, 2003). However, a second element reported by Papp (2011) is that for the specific case of a 2x2 symmetric matrix, $X = \begin{bmatrix} x_0 & x_1 ; & x_1 & x_2 \end{bmatrix}$, one can write that

$$X \text{ is p.s.d.} \Leftrightarrow x_0 \geq ||(x_1, \ldots, x_n)||^2 \quad (6)$$

In other words, positive semi-definiteness of a symmetric 2x2 matrix is guaranteed by a norm-based constraint on its elements. The norm-based inequality constraint in Eq. (6) describes a so called second-order cone (SOC) or Lorentz cone. Positive semi-definiteness of 1x1 matrices, $X = [x_0]$, reduces to:

$$X \text{ is p.s.d.} \Leftrightarrow x_0 \geq 0 \quad (7)$$

This means that the fitting of a non-negative polynomial of degree zero (0, constant) to three (3, cubic polynomial) can be cast as the search for its optimal parameters, p_k, subject to the equality constraints (Eqs. (4) and (5)) and inequality constraints (Eqs. (6) and (7)). Furthermore, if optimality is defined by means of a convex function of the parameters, then the problem reduces to a SOCP. SOCPs are special cases of SDPs and are easier to solve than general SDPs by means of specific interior-point algorithms (Alizadeh & Goldfarb, 2003).

Because spline functions and their derivatives are piece-wise polynomials, the above strategy can be used for SCS fitting. Indeed, by applying non-negative (non-positive) constraints to the piecewise polynomial presentation of the spline and its derivatives one can specify the signs for the function and its derivatives over any interval within the function domain. SCS fitting with non-negative or non-positive constraints on the function value and/or its derivatives is thus equivalent to solving the problem:

$$\text{minimize} F(\mathbf{y}, \mathbf{c}) \quad (8)$$

subject to:

$$s_{e,k} \cdot f^{(k)}(t, \mathbf{c}) \geq 0 | t \in [t_{e,1}, t_{e,2}] \wedge s_{e,k} \in \{-1, 1\} \quad (9)$$

with:

t : spline function argument
$\mathbf{c} = (c_i)_{i=1\ldots m+n-1}$: vector of spline coefficients
$\mathbf{y} = (y_j)_{j=1\ldots l}$: time series vector
$F(\mathbf{y}, \mathbf{c})$: convex objective function
$f^{(k)}(t, \mathbf{c})$: k th derivative of the spline function
$s_{e,k}$: sign of$k$ th derivative in$e$ th episode
$t_{e,1}$: left-hand side endpoint of the$e$ th episode
$t_{e,2}$: right-hand side endpoint of the$e$ th episode
m : number of knots
n : degree of the spline function

We note the knot locations of the spline as follows $a_1, \ldots, a_i, \ldots, a_m$ with

$$a_i < a_{i+1} \quad (10)$$

Depending on the order k, the constraints imply non-strict positivity ($k=0$), isotonicity ($k=1$), or convexity ($k=2$) of the fitted function. Each instance of Eq. (9) defines an infinite number of constraints as t is continuous in the interval $[t_{1,e}, t_{2,e}]$. Each of these constraints are linear in the spline coefficients $\mathbf{c}$. As long as long as $n-k \leq 3$ for all instances of Eq. (9), then these infinite number of constraints can be converted into a finite number of linear equalities and SOCs. We assume that this is satisfied for the remainder of the text so that all instances of Eq. (9) can be solved as an SOCP.

To reformulate the infinite number of constraints of Eq. (9) into a finite number of SOCs, one first defines the ordered set of arguments consisting of (1) the two interval bounds over which the shape constraint is specified and (2) all the knots of the spline function inside this interval as follows:

$$\mathbf{b} = (b_j)_{j=1\ldots r+2} = \begin{bmatrix} t_{e,1} & a_{q+1} & \ldots & a_i & \ldots & a_{q+r} & t_{e,2} \end{bmatrix} \quad (11)$$

with:

$$t_{e,1} < a_{q+1} < \ldots < a_i < \ldots < a_{q+r} < t_{e,2} \quad (12)$$

Then, Eq. (9) can be rewritten into $r+1$ separate equations:

$$\forall j \in [1 \ldots r+1] : s_{e,k} \cdot f^{(k)}(t, \mathbf{c}) \geq 0 | t \in [b_j, b_{j+1}] \wedge s_{e,k} \in \{-1, 1\} \quad (13)$$

The intervals $[b_j, b_{j+1}]$ do not contain any of the spline knots in their interior so that each of the $r+1$ equations corresponds to the non-negativity or non-positivity of a single polynomial of degree $n-k$. As a result, each of the instances in Eq. (13) correspond to a set of two equations (Eqs. (4) and (6) or Eqs. (5) and (7), respectively). As an example, consider that a non-negative constraint is applied to the function value of spline of degree 3. Then Eqs. (4) and (6) are written explicitly as follows:

$$\forall j \in [1 \ldots r+1] : \quad (14)$$

$$\begin{aligned}
X_j &= \begin{bmatrix} x_{j,0} & x_{j,1} \\ x_{j,1} & x_{j,2} \end{bmatrix} \\
Y_j &= \begin{bmatrix} y_{j,0} & y_{j,1} \\ y_{j,1} & y_{j,2} \end{bmatrix} \\
p_{j,0} &= \mathbf{g}_{q+j,0} \cdot \mathbf{c} = -b_j \cdot x_{j,0} + b_{j+1} \cdot y_{j,0} \\
p_{j,1} &= \mathbf{g}_{q+j,1} \cdot \mathbf{c} = 2 \cdot (-b_j \cdot x_{j,1} + b_{j+1} \cdot y_{j,1}) + (x_{j,0} - y_{j,0}) \\
p_{j,2} &= \mathbf{g}_{q+j,2} \cdot \mathbf{c} = -b_j \cdot x_{j,2} + b_{j+1} \cdot y_{j,2} + 2 \cdot (x_{j,1} - y_{j,1}) \\
p_{j,3} &= \mathbf{g}_{q+j,3} \cdot \mathbf{c} = x_{j,2} - y_{j,2} \\
x_{j,0} + x_{j,2} &\geq ||(x_{j,0} + x_{j,2}, 2 \cdot x_{j,1})||^2
\end{aligned}$$

The vectors $\mathbf{g}_{q+j,k}$ are defined as the sets of linear coefficients to project the spline basis coefficients, $\mathbf{c}$, onto the piece-polynomial basis coefficients of degree k in interval $q+j$. This projection can easily be obtained analytically (de Boor, 1978; Ramsay & Silverman, 2005).

A solution to the SOCP represented by Eqs. (8) and (9) can be found under the following conditions:

- The objective function is convex in the spline coefficients.
- Non-negative, isotonic, or convex shape constraints are applied for spline functions of maximal degrees 3, 4 and 5 respectively.

This further allows to:

- Apply non-negative counterparts of the above-mentioned constraints, i.e., non-positive, antitonic, and concavity constraints.
- Apply shape constraints over the whole or intervals of the function domain.
- Apply mixed shape constraints, e.g., non-negativity/non-positivity, monotonicity, and monocurvature or any subset thereof, each applied over the same or different intervals of the function domain.

The problem described by Eqs. (8) and (9) is limited as follows:

Limitation 1 All considered constraints in Eq. (9) are inequality constraints, thus implying a non-negative or non-positive value for the derivatives. Equality constraints are not considered (zero value ($k=0$); flat trend ($k=1$); linear trend ($k=2$)).

Limitation 2 The intervals over which the constraints are specified are considered given. The optimal identification of the interval endpoints is not considered.

The first one is not severe and tackled in the next paragraph. The second limitation is more challenging and is tackled in Section 2.3.

2.2.2. Shape generalization

We generalize the existing method in Papp (2011) first by allowing the use equality constraints on any of the derivatives up to degree n. The addition of equality constraints is quite trivial. Using earlier definitions, such a constraint is written as:

$$f^{(k)}(t, \mathbf{c}) = 0 | t \in [t_{e,1}, t_{e,2}] \wedge s_{e,k} = 0 \quad (15)$$

Such a constraint specifies an interval in which the fitted function exhibits a zero-valued derivative of degree k. As before, Eq. (15) defines an infinite number of constraints as t can take an infinite number of values. To reformulate this equation in a finite number of constraints it is sufficient that each piece-wise polynomial is constrained individually. Mathematically, one writes:

$$\forall j \in [1 \ldots r+1] : f^{(k)}(t, \mathbf{c}) = 0 | t \in [b_j, b_{j+1}] \wedge s_{e,k} = 0 \quad (16)$$

Furthermore, for a polynomial to be zero over a given interval it is necessary and sufficient that all its coefficients are zero. Therefore, Eq. (16) is made more explicit as follows:

$$\forall j \in [1 \ldots r+1], \forall k \in [0 \ldots n-k] : p_{j,k} = \mathbf{g}_{q+j,k} \cdot \mathbf{c} = 0 \quad (17)$$

Importantly, the provided generalization only requires a set of linear equality constraints to be added to Eq. (9).

The complete problem of fitting a spline function subject to a set of shape constraints formulated as a QR is now defined by Eqs. (1)–(3), (8)–(9), and (15). This complete problem remains a SOCP which includes linear equality constraints, linear inequality constraints, and SOC constraints. It is slightly more general than

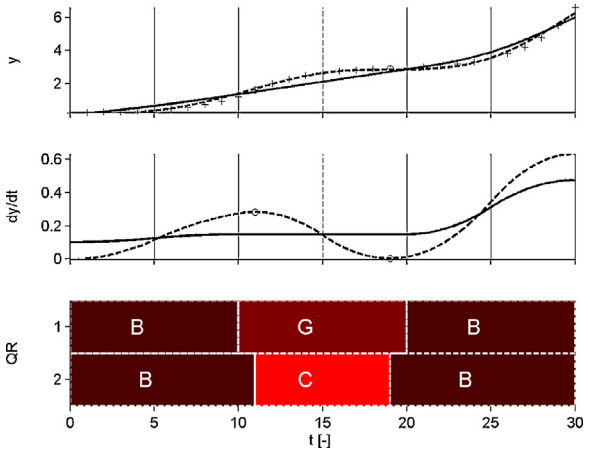

Fig. 1. Two cubic spline functions fitted subject to a BCB shape constraint. Top: simulated data (+), spline functions (full,dashed); Middle: Derivative of the functions (full,dashed); Bottom: resulting qualitative representations (QR).

the original problem (Papp, 2011). Some practical restrictions still apply. These are described in the next paragraphs.

2.2.3. Remaining restrictions

Restriction 1 Discontinuities in the spline function or its derivatives of low order ($k \leq n$), corresponding to multiple knots in the spline, are not permitted. For instance, an FC sequence requires a discontinuity in the first and second derivative at the endpoint shared by two primitives while it should otherwise be continuous in these derivatives.

Restriction 2 There are maximally $n-k$ changes in the sign of the kth derivative between two consecutive knots of the spline. The kth derivative of a spline function is a piece-wise polynomial of degree $n-k$. As a result, the kth derivative can only be zero-valued in maximally $n-k$ distinct locations (roots of the polynomial) unless all the polynomial coefficients are zero. It follows that the application of a set of shape constraints which imply more than $n-k$ changes in the sign of the kth derivative between two consecutive knots will effectively constrain this derivative to be zero over the entire interval. For this reason, the number of implied changes of sign in the kth derivative between two consecutive knots is restricted to be smaller than one for all practical purposes.

To demonstrate the value of this restriction consider that a cubic spline ($n=3$) is fit with a BCB shape constraint over an interval defined by two consecutive knots, $[a_i, a_{i+1}]$. This is demonstrated in Fig. 1 for a simulated data series composed of exponential basis functions which is known to be of BCB shape and with internal episode endpoints (inflection points) at argument values 11 and 19. A cubic spline is fitted with internal knots at 5, 10, 20, and 25 and subject to the BCB shape constraint with the known internal endpoints (11 and 19). This means that the second derivative is forced to be zero in two distinct locations in the second knot interval. However, the second derivative is linear in the argument ($n-k=1$) over the knot interval $[a_i, a_{i+1}]$ and thus will be zero over the whole interval. As such, a linear G episode results in the second knot interval rather than the intended sequence of BCB episodes, leading to a BGB shape instead with internal episode endpoints at 10 and 20. This is easy to see from the plot of the spline function's first derivative.

Naturally, it is possible to add more knots to a spline function so to accommodate more episode endpoints in particular intervals of the spline argument range. This is demonstrated in Fig. 1 by adding an additional knot at argument value 15. As can be observed, this leads to the desired fit which matches the intended BCB shape. Such an ad hoc placement of additional knots by human interaction may be prohibitive for large-scale, on-line, or otherwise repetitive applications. Fortunately, a wide range of strategies for automatic knot placement exist (see e.g., Cox, Harris, & Jones, 1990; Friedman, 1991; Hölzle, 1983; Jupp, 1978). Alternatively, a knot may be placed in each data point leading to a so called smoothing spline. This permits one inflection point to be placed between each pair of consecutive knots. Similarly, this allows two extrema and three zero-crossings between each pair of consecutive data points. This is likely to suffice for most practical applications and avoids an algorithmic search for optimal knot placement.

Restriction 3 The endpoints of episodes implying equality constraints (E, F and G primitives) should be knots. If one constrains a spline function value or any of its derivatives to be zero over a non-empty interval with bounds $[t_{e,1}, t_{e,2}]$, then this constraint is automatically satisfied over the interval $[a_q, a_r]$ defined by two knots, a_q and a_r, and which includes $[t_{e,1}, t_{e,2}]$:

$$[a_q, a_r] \quad \text{with} a_q \leq t_{e,1} < a_{q+1} \wedge a_{r+1} < t_{e,2} \leq a_{r+1} \tag{18}$$

This is true because a polynomial which is zero-valued over a non-empty interval of its argument range is automatically zero-valued of its whole argument range. As the interval satisfying an equality constraint is always bounded by two knot locations, episodes implying such constraints are restricted to be defined by means of knots locations as interval bounds for all practical purposes.

2.3. Identifying a Qualitative Representation (QR) conditional to a given Qualitative Sequence (QS)

The above developments permit fitting of a spline function subject to shape constraints formulated as a qualitative representation (QR). Such a QR is defined as a contiguous set of episodes, each given as an interval of the spline function argument range for which a particular set of constraints (primitive) is enforced. However, in the more general case, one does not know the (precise) endpoints of these episodes and only the qualitative sequence (QS) is given. It is therefore of interest to obtain the optimal episode endpoints so as to obtain the best spline function fit which is constrained to be of the given shape (QS, Eq. (3)). For each of these primitives, proper endpoints are searched for to obtain the episodes, $t_{e,1}$ and $t_{e,2}$, $e=0\ldots n_e-1$. The left-side (right-side) endpoint of the first (last) episode is known to be equal to the first (last) knot of the spline function:

$$t_{1,1} = a_1 \tag{19}$$

$$t_{n_e,2} = a_m \tag{20}$$

Furthermore, contiguity means that for each pair of contiguous episodes the right endpoint for the left episode is the left endpoint for the right episode (Eq. (2)). This leaves $n_e - 1$ undefined endpoints shared by pairs of consecutive episodes and, as above, referred to as transitions. We use the following shorter notation for these transitions:

$$t_e = t_{e,2} \tag{21}$$

Finding these transitions is a non-linear problem for which no analytical solution exists. In this work, we are interested in finding the globally optimal values for these transitions and it is for this reason that the B&B algorithm is used in this work. In the next sections (Sections 2.3.1 and 2.3.2) the basis of this algorithm, heuristic rules, and implementation details are described. The following sections (Sections 2.3.3 and 2.3.4) deal with the computation of lower and upper bounds for use within the B&B algorithm.

2.3.1. Branch and Bound (B&B) algorithm

B&B algorithms are a set of deterministic, global optimization algorithms for non-linear programs (NLPs) and have been developed extensively to solve particular problems over the years (Floudas & Gounaris, 2009; Lawler & Wood, 1966; Mitten, 1970). For gentle introductions to global optimization see Parker and Rardin (1988) and Forst and Hoffmann (2010). The basic tenet of B&B lies in a divide-and-conquer strategy by which the variable space is divided into smaller sets for which lower and upper bounds of the objective function (F_L, F_U) are computed. This process can be visualized by a tree starting from the complete variable space (*root node*) which is split into smaller subsets (*branching*). Each of these subsets are branched further into smaller sets (*child nodes*). Child nodes which are not split yet at a given time during algorithm execution are called *leaf nodes*.

If the optimization problem is a minimization problem, then all the (feasible) solutions that lie within a given set are guaranteed to have an objective function value which is not lower than the computed lower bound for that set. In addition, at least one (feasible) solution within a given set is known to have an objective function value which is not higher than the upper bound. As soon as one obtains a set, $\mathcal{A}$, for which the lower bound is higher than the upper bound of a second set, $\mathcal{B}$, then one can ignore $\mathcal{A}$ since $\mathcal{B}$ contains at least one solution which is better than all the solutions in $\mathcal{A}$. Therefore, $\mathcal{A}$ is known not to have the global optimum for the optimization problem and can thus be ignored further in search for the global optimum. The process by which such sets (leaf nodes) are excluded for further exploration (branching) is called *fathoming*. Fathomed leaf nodes are said to be *dead*; other leaf nodes remain *alive*. By means of fathoming, one can avoid detailed and long-during exploration of large subsets of the variable space. Quite naturally, the B&B algorithm requires that one is able to compute the lower and upper bounds. Furthermore, the B&B algorithm will converge to the global optimum if (1) the bounds are provably valid and (2) the lower bound is provably lower or equal to the upper bound. For fast convergence of the B&B algorithm, the computed lower bound should be as close as possible to the optimal objective function. In the general case, this implies a bargain between efficient execution of the B&B algorithm and efficient computation of the lower bound.

2.3.2. Heuristics and practical implementation

The particular implementation of B&B algorithm for this work is fully characterized by the choices described in the next paragraphs. Note that other choices are possible (Forst & Hoffmann, 2010). Such choices may affect the speed of convergence and are usually based on heuristics and/or knowledge of the mathematical problem at hand. However, these do not affect guarantees on convergence of the algorithm.

Variable subset The subsets are defined as rectilinear polyhedra (e.g., rectangle for two-variable problem; parallelepiped for three-variable problem). Mathematically such a subset, $\mathcal{T}$, is defined as:

$$\mathcal{T} = \{t | l_e \leq t_e \leq u_e, e = 1 \ldots n_e - 1\} \tag{22}$$

with l_e and u_e lower and upper limits defining the polyhedral set.

Branching A leaf node (subset) is always branched into two new nodes (two subsets) by dividing the subset in two equal halves along one of the decision variables (t_e).

Leaf selection In our case, the leaf node that has the lowest lower bound (F_L, see below) among the leaf nodes that are alive is selected for branching.

Variable selection The selected variable for subset division is always the one corresponding to the longest edge of the polyhedron which defines the subset corresponding to the leaf node.

Stopping criterion The algorithm is stopped if (1) only one node remains alive and (2a) all values t_e are found within desired precision (i.e., the subset is small enough) or (2b) if the difference between upper bound and lower bound is smaller than a preset tolerance. In this study, this tolerance is set to zero. This means that the (2b) condition is only met if the lower and upper bound are exactly the same.

The B&B algorithm as applied here is implemented in Matlab (The MathWorks Inc., 2010). Its use for SCS fitting relies on an existing Matlab toolbox for Functional Data Analysis (Ramsay & Silverman, 2002) and MOSEK (Andersen & Andersen, 2000) as the optimization software for SOCPs. The implementation as used for this work is available in supplementary materials and also allows to use CVX (Grant & Boyd, 2011) for optimization of the SOCPs. The following description summarizes the B&B algorithm implementation:

1 **Initialization:** Define the *current node* as a *leaf node* and label it *alive*. Compute the associated upper and lower bounds.
2 **Branching:**
  (a) Variable selection: Select the variable with maximum range in the current set
  (b) Split set: Split the current node in two new *leaf nodes* by halving the current set along the selected variable. Relabel the current set as a *branch node* and each of the newly generated *leaf nodes* as *alive*.
3 **Bounding:** For each new *leaf node*:
  (a) Find a feasible candidate solution, if any (Section 2.3.3)
  (b) If a feasible solution is found, then:
    i Upper bound: Compute the upper bound, F_U (Section 2.3.3)
    ii Lower bound: Compute the lower bound, F_L (Section 2.3.3)
    iii Shape verification: Improve the upper bound when possible based on shape evaluation (Section 2.3.4).
  (c) Else (infeasible set), both bounds are set to infinity
    i Upper bound: $F_U = \infty$
    ii Lower bound: $F_L = \infty$
4 **Fathoming:** Relabel any *alive leaf node* which has a lower bound higher than the upper bound of any other *alive leaf node* as a *dead leaf node*.
5 **Node selection:** Select the *alive leaf node* with the lowest value for the lower bound as the *current node*.

6 **Iteration / Termination:**
(a) If (1) the *current node* is the only *alive leaf node* and (2a) the range of each variable is below the preset minimal precision or (2b) the difference between its upper bound and lower bound is below is smaller than the preset tolerance, then terminate the algorithm and report the upper bound solution for this set.
(b) Else, go to 2.

2.3.3. Bounds to the objective function

Finding a feasible solution. The computation of the lower and upper bound only differs in the applied constraints (Eqs. (9) and (15)). To obtain the bounds for the objective function, one first tries to find a feasible set of values for the transitions, t_e. Feasibility means that the proposed set belongs to the considered polyhedron (Eq. (22)) and the ordering of the transitions is (non-strictly) preserved:

$$t_e \leq t_{e+1} \tag{23}$$

If a feasible set of values exists, one such set can be found through solving the following linearly constrained and convex quadratic program (QP):

$$\min_{t_e} \sum_e (t_e - u_e)^2 + \sum_e (t_e - l_e)^2 \tag{24}$$

$$\begin{aligned} t_e &\leq t_{e+1} \\ t_e &\leq u_e \\ l_e &\leq t_e \end{aligned}$$

Thus, a feasible point is found by finding a point in the considered set which minimizes the sum of the squared distances from this point to each surface of rectilinear set while preserving the order of the transitions. Whether or not this QP is feasible can be verified easily with commercial solvers as used in this work.

Feasible case – upper bound. We discuss the case where a feasible set of values for t_e is found first. In this case, an upper bound for the objective function is found by evaluating the constraint equations (Eqs. (9) and (15)) with the proposed feasible set of values for the transitions, t_e:

$$s_{e,k} \cdot f^{(k)}(t, \mathbf{c}) \geq 0 | t \in [t_e, t_{e+1}] \wedge s_{e,k} \in \{-1, 1\} \tag{25}$$

$$f^{(k)}(t, \mathbf{c}) = 0 | t \in [t_e, t_{e+1}] \wedge s_{e,k} = 0$$

In this case, Eq. (25) describes an (infinite) set of linear equality and inequality constraints in the spline coefficients, $\mathbf{c}$. This means that the values for $\mathbf{c}$ are constrained to lie in a convex subset of $\mathbb{R}^{m+n-1}$, noted $\mathcal{C}_U$:

$$\mathbf{c} \in \mathcal{C}_U \subseteq \mathbb{R}^{m+n-1} \tag{26}$$

Because a feasible point is evaluated, the globally optimum value for objective function found for values t_e within the set described by Eq. (22) is indeed equal to or lower than the evaluated objective function value:

$$F_{OPT} \leq F_U \tag{27}$$

As such, the computed F_U is a valid upper bound.

Feasible case – lower bound. The lower bound is computed by imputing the subset boundaries into Eqs. (9) and (15) as follows:

$$s_{e,k} \cdot f^{(k)}(t, \mathbf{c}) \geq 0 | t \in [u_e, l_{e+1}] \wedge s_{e,k} \in \{-1, 1\} \tag{28}$$

$$f^{(k)}(t, \mathbf{c}) = 0 | t \in [u_e, l_{e+1}] \wedge s_{e,k} = 0$$

This means that all constraints evaluated at a function argument value which belongs to the considered endpoint set ($\mathcal{T}$) are excluded. Since it holds that:

$$l_{e+1} \leq t_{e+1} \tag{29}$$

$$t_e \leq u_e$$

one can write:

$$[u_e, l_{e+1}] \subseteq [t_e, t_{e+1}] \tag{30}$$

The consequence of this relationship is that all inequality and equality constraints applied for the lower bound problem (Eq. (28)) are included for any specific solution satisfying Eq. (22). As a result, the set of coefficient vectors, $\mathbf{c}$, defined by Eq. (25) for any feasible set of values of t_e, $\mathcal{C}_U$, is a subset of the set of coefficient vectors defined by Eq. (28), $\mathcal{C}_L$:

$$\mathbf{c}_U \in \mathcal{C}_U \subseteq \mathcal{C}_L \subseteq \mathbb{R}^{m+n-1} \tag{31}$$

Because (1) the objective function for both lower and upper bound (Eq. (8)) is exactly the same and (2) the feasible set of coefficients for the upper bound is a subset of the feasible set of coefficients for the lower bound, the following is true for any feasible set defined by Eqs. (22) and (23):

$$F_L \leq F_U \tag{32}$$

Indeed, no solution satisfying Eqs. (22) and (23) can be found with an objective function lower than F_L.

Infeasible case. Now consider the case where no feasible solution satisfying Eqs. (22) and (23) could be found. In this case the problem is infeasible and both bounds are set to infinity ($F_U = F_L = +\infty$). Also in this case, both bounds are valid and satisfy Eq. (32).

Notes on the bounding procedures. As a result of the above, the lower bound objective function value is equal to or lower than any possible value it can take for the values of t_e in the considered set (Eq. (22)). Since the global optimum corresponds to one choice for the values t_e within this set, this proves the validity of the lower bound procedure:

$$F_L \leq F_{OPT} \tag{33}$$

The lower and upper bounding procedures for the feasible case consist of the solution of a SOCP which result in the optimal spline coefficients conditional to the applied shape constraints. SOCPs are convex problems and are therefore relatively easy to solve, e.g., by means of Interior Point (IP) methods (Alizadeh & Goldfarb, 2003). As a result, the B&B algorithm and the presented bounding procedures allow to compute the globally optimal solution of the complete problem, including both the spline coefficients and the episode endpoints. Note that the optimization problem is not convex in the episode endpoints, thereby requiring a slower non-linear programming (NLP) method such a B&B for global optimization of these parameters.

2.3.4. Improvement of the upper bound by shape verification

In certain cases the lower bound solution will satisfy the intended QS, even though not all of the implied constraints are explicitly included in the problem specification. In such case, the lower bound is also an upper bound for the considered set and the obtained solution represents the global optimum within the considered set. There are two possible cases:

Case 1 – Known QS satisfaction The number of zero-crossings, extrema, and inflection points between two consecutive knots is limited in certain

cases as indicated in Section 2.2.3. For example, there can only be a single inflection point between two knots. This means that if the considered subset specifies that the inflection points, t_e, each lie within an interval $[l_e, u_e]$ which is contained within an knot interval $[a_i, a_{i+1}]$:

$$\forall e, \exists i : [l_e, u_{e+1}] \subseteq [a_i, a_{i+1}] \quad (34)$$

then the lower bound solution satisfies the implied shape constraint automatically. One can evaluate the exact argument value corresponding to such inflection point, which specifies the upper bound solution completely. Therefore the upper bound, F_U, can be set equal to the computed lower bound, F_L. The same can be done for extrema and zero-crossings if the sign of the higher-order derivatives is constant over the specified knot interval, following restrictions in Section 2.2.3.

Case 2 – Evaluated QS satisfaction If case 1 does not apply, one can evaluate the shape of the spline corresponding to the lower bound by computing the roots corresponding to zero-crossings, extrema, and inflection points. In some cases, the evaluated sequence (QS_{eval}) will match the desired QS exactly. To assess whether this is the case, one evaluates the argument values corresponding to zero-crossings, extrema, and inflection points by finding the roots, t_s, corresponding to the zero-crossing of the piece-wise polynomials which represent the function value, first derivative, and second derivative within each of the intervals $[l_e, u_e]$. If each of these roots are unique and satisfy Eqs. (22) and (23), then Eq. (25) is evaluated with:

$$t_e = t_s \quad (35)$$

If one or more roots are not unique, then the original upper bound is kept. Note that the solution t_s represents one particular point in the subset defined by Eq. (22). As such, all assessments about the bounding procedures remain valid. Furthermore, the transitions used in Eq. (25) for the upper bound are now the same as those derived from the lower bound solution obtained with Eq. (28). This means that the obtained coefficients, **c**, are the same and thus:

$$F_L = F_R \leq F_U \quad (36)$$

with F_L and F_U the original bounds and the F_R the improved upper bound. Since the improved upper bound is the same to the lower bound, this also means that it is unnecessary to branch the particular node further. Indeed, the upper bound solution is the best solution within the subset since no better solution can be found. This means that one can obtain the exact solution for the values of t_e in a finite number of steps if the following is satisfied:

- The specification of an endpoint, t_e, implies (1) a change in the sign of a derivative, say the kth derivative with degree $n-k$, at t_e and (2) the sign of each higher derivative ($n-k+1$th until nth) is known to be the same (either non-negative or non-positive) left and right of the considered endpoint.

For the specific case of a cubic spline ($n=3$), this can be interpreted as follows:

- Condition 1: The endpoint, t_e, implies a change in sign of the function value at t_e and the signs of the first and second derivative are known (+, 0, or −) and the same left and right of t_e (zero crossing). This is true for any endpoint shared by two contiguous episodes with a sequence of primitives of the form (1) X^+X^-, X^-X^+ where X can be any triangular primitive (A to G) or (2) $F^\circ D^-$, $F^\circ B^+$, A^+F°, and C^-F°.
- Condition 2: The endpoint, t_e, implies a change in sign of the first derivative at t_e and the sign of the second derivative is known (+, 0, or −) and the same left and right of t_e (extremum). This is true for any endpoint shared by two contiguous episodes with any of following sequence of primitives: AB, CD, AF, FD, CF, and FB.

- Condition 3: The endpoint, t_e, implies a change in sign of the second derivative at t_e (inflection point). This is true for any endpoint shared by two contiguous episodes with any of following sequence of primitives: AD, DA, BC, CB, AN, NA, BN, NB, PD, DP, PC, CP, PN, and NP.

3. Results

We use three examples to demonstrate the developed method. In the first two examples a Shape Constrained Spline (SCS) function is fit to a data series. The third example demonstrates the use of SCS function fitting as part of a diagnosis strategy based on qualitative analysis.

3.1. Titanium data set

3.1.1. Case study and previous work.

The Titanium data set was reported originally in de Boor (1978) and has been used to demonstrate shape-constrained fitting in Turlach (2005). In our study, the same objective function as in Turlach (2005) is applied. It is the least-squares lack-of-fit measure with L^2-norm regularization of the derivatives:

$$J(y,c) = \sum_{j=1}^{n}\left(\frac{y_j - f(x_j,\mathbf{c})}{\sigma}\right)^2 + \sum_{k=0}^{n}\lambda_k \int_{a_1}^{a_m} (f^{(k)}(u,\mathbf{c}))^2 du \qquad (37)$$

with:

$\mathbf{x} = (x_j)$: vector of argument values for the data series
$\mathbf{y} = (y_j)$: vector of observed values for the data series
λ_k : regularization parameter for k-th derivative
σ : measurement error standard deviation
$f(t,\mathbf{c})$: spline function

This objective corresponds to a maximum a posteriori (MAP) likelihood fit. This correspondence is true if (1) the measurement errors are assumed to be distributed with zero mean and standard deviation σ and (2) a prior distribution on the coefficients is assumed which favors a smooth function. In this study, σ and λ_k are set to fixed values as follows: $\sigma = 1$; $\lambda_0 = 0$; $\lambda_1 = 0$; $\lambda_2 = 0$; $\lambda = 10^{-7}$. This leads to the same objective function as in Turlach (2005). The use of priors as applied here is also known as regularization. This can be motivated on the basis of smoothness objectives (Hastie, Tibshirani, & Friedman, 2001), which can be formulated as the minimization of empirical risk (Vapnik, 1995). In such case, the regularization parameters λ_k are considered meta-parameters which are to be optimized. Alternatively, regularization also arises as a consequence of (Bayesian) prior beliefs (MacKay, 2003). In this case, the regularization parameters are fixed a priori. We consider the latter case in this study.

This objective function is convex quadratic in the spline coefficients. Three cubic spline fits are shown in the top panel of Fig. 2. Visual discrimination between the three fitted function is hard on the basis of these function plots. The bottom panel permits a clearer interpretation based on the first derivatives of the same fitted functions. The first result was reported already in Turlach (2005) and consist of an interpolating cubic spline without shape constraints (QS = Q). The resulting shape of the first spline fit is fairly complex as is evident from the multiple zero-crossings of the first derivative (many inflection points). The second cubic spline is constrained to be convex in the (closed) intervals [595, 835] and [955, 1075] (QS = PQP) as in Turlach (2005). Note that the SOCP based method of Papp (2011) as described in Section 2.2 is applied and not the method developed in Turlach (2005). This second spline fit results in a ABCDAB sequence with the following transition locations: 607.59, 880.22, 897.99, 911.77 and 1027.28. This means that two episodes with a negative and positive sign for the 1st derivative are observed at the beginning, respectively end, of the fitted function. The third fit is obtained through the method provided in this paper and discussed in detail below.

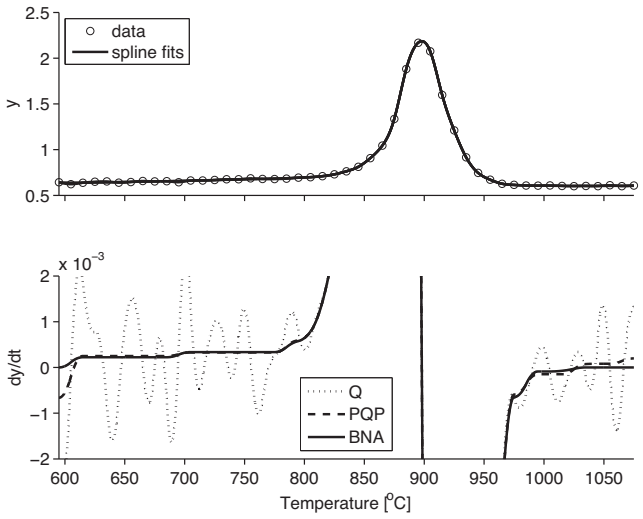

Fig. 2. Results for the Titanium data set. Top: data and three different spline fits. Bottom: smoothing spline derivative without constraints (Q), convex shape constraints (PQP), and mixed shape constraints (BNA).

3.1.2. Demonstration of bounding procedures.

The bounding procedures are demonstrated first. To this end, the fitted spline is constrained to consist of three episodes, respectively of (1) a convex isotonic, (2) a concave, and (3) a convex antitonic shape. The QS is thus BNA and the location of two inflection points (transitions) are to be optimized. For demonstration purposes, the transitions are considered to be in the intervals [675, 755] and [835, 915], respectively. Solving the quadratic program to find a feasible solution (Section 2.3.3) leads to transitions at 715 and 875. Using these transition values leads to the fit in Fig. 3. The corresponding

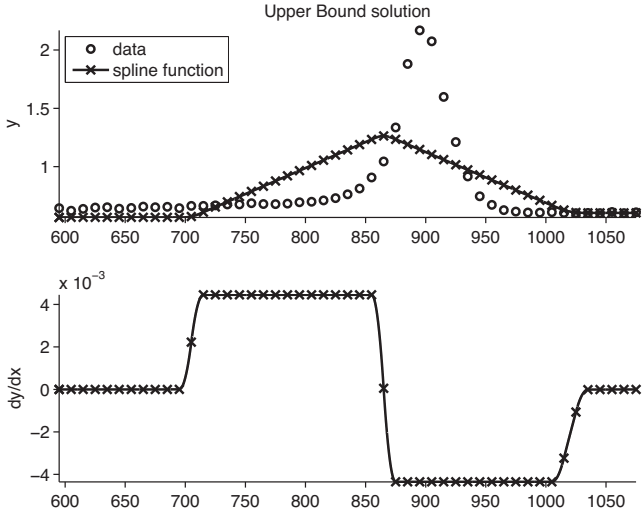

Fig. 3. Upper bound solution for a BNA shape constrained fit. Top: data and fitted spline. Bottom: spline derivative.

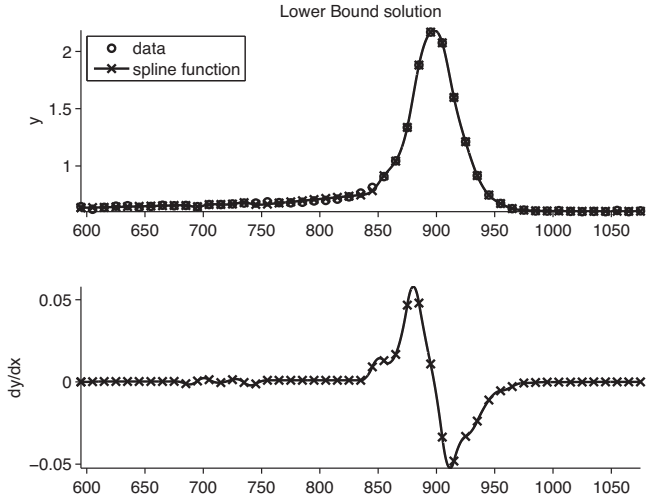

Fig. 4. Lower bound solution for a BNA shape constrained fit. Top: data and fitted spline. Bottom: spline derivative.

upper bound value (F_U) is 4.0886. This is a rather high value as might be expected from the visibly poor fit of the resulting spline function. However, one can visually confirm that the fitted spline function satisfies the shape constraint. The first derivative increases (non-strictly convex) until 715, then decreases until 875 only (non-strictly concave) to increase again after that (non-strictly convex). Moreover, the derivative is positive before 715 (non-strictly isotonic) and negative after 875 (non-strictly antitonic).

To obtain the corresponding lower bound solution, one removes all shape constraints over the intervals defined by the considered set, namely [675, 755] and [835, 915] (Section 2.3.3). This means that a BQNQA shape is fitted with transitions at 675, 755, 835 and 915. Fig. 4 shows the resulting fit. The corresponding lower bound value (F_L) is 0.0033. This is a low value indicating a good fit of the resulting spline function, thus demonstrating the relaxation obtained by removing shape constraints. However, the resulting shape is not a BNA shape as desired. Indeed, the first derivative has multiple local maxima – not one, as desired – in the interval [675,755] and multiple local minima in the interval [835,915].

3.1.3. Demonstration of the B&B algorithm.

The demonstrated bounding procedures are now used within the B&B algorithm (Section 2.3.2). The B&B algorithm was run to identify the optimal locations of the two inflection points at the intersection of these episodes. The optimal solution is found after 26 branching steps. This means that 53 nodes of the solution tree are explored, equivalent to solving 106 SOCPs (one for the lower and upper bound respectively). The executed branching steps are displayed in Fig. 5. The optimized location of the inflection points are at 880.219 and 911.771 respectively.

Now return to Fig. 2 where the third fit is the SCS constrained with a QR consisting of the BNA shape (QS) and the obtained optimal values for transitions. It is easy to verify that the BNA sequence implies the existence of a single maximum in the interior of the N-episode. The resulting shape is thus a BCDA sequence. This eliminates the first A and last B episodes as found for the second fit (with PQP shape). The location of the maximum is found at 898.00.

3.2. Retrieving a known function

3.2.1. Case study

The second example is aimed at demonstrating that the B&B algorithm can be used to estimate a known function as well as the true locations of corresponding episode endpoints. To this end,

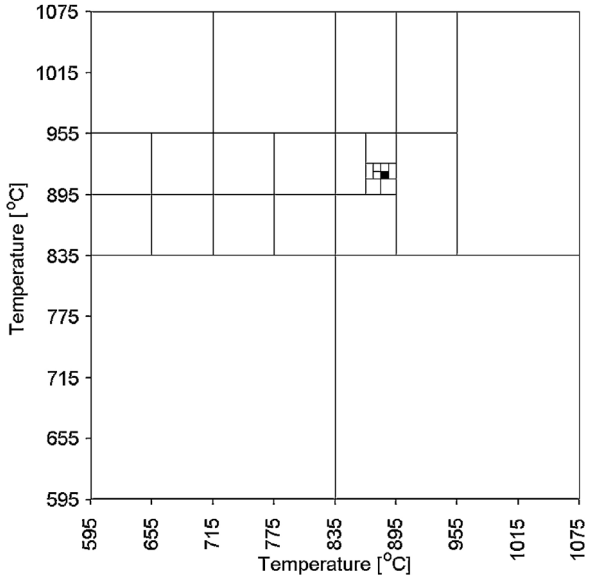

Fig. 5. Visualization of the B&B algorithm for the Titanium data and BNA sequence. Each vertical (horizontal) line represents a split of a subset along the first (second) transition. The black square represents the only remaining live node at termination of the algorithm.

artificial data is generated by sampling the following equation in the range 0–3:

$$y = \begin{cases} 2.x^3 + 1 & \text{if } 0 \le x \le 1 \\ -10.x^3 + 36.x^2 + 36.x + 13 & \text{if } 1 < x \le 2 \\ 8.x^3 - 72.x^2 + 180.x - 131 & \text{if } 2 < x \le 3 \end{cases} \quad (38)$$

It can be verified that the above equation corresponds to a cubic spline with interior knots located at $x = 1$ and $x = 2$. In addition, it is a natural spline as the second derivative is zero in the argument values $x = 0$ and $x = 3$. The polynomial coefficients of this function were chosen so that the resulting function has a $B^+C^+D^+D^-$ shape and is characterized by an inflection point, a maximum, and a zero-crossing at the argument values 1.20, 1.69 and 2.28 respectively. The above function is sampled at equal intervals of 0.1 from 0 to 3, leading to a series of 31 data points. Fig. 6 displays the sampled data points.

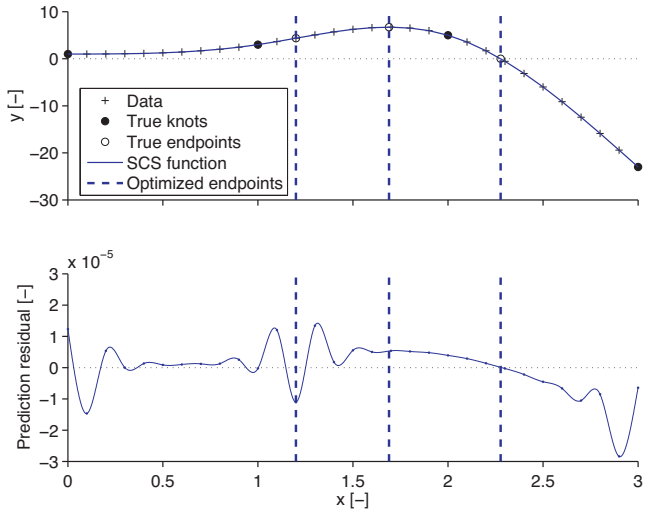

Fig. 6. Results for the known function data set. Top: data points, true knots, true transitions, Shape Constrained Spline (SCS) function fit, and optimized transitions. Bottom: Prediction residual between fitted function and true function.

3.2.2. Results

An SCS function is fitted to the optimized data by means of the B&B algorithm. The function is a natural cubic spline with knots located in the argument of each data point and is determined by 31 coefficients. The applied qualitative sequence (QS) is the $B^+C^+D^+D^-$ sequence and the objective function is the sum of squares of residuals between sampled data points and fitted function evaluations in the same arguments. Since the data-generating function and the fitted function are of the same type (natural cubic spline) and the knots of the fitted function include all of the knots corresponding to the data-generating function, one expects that a perfect function fit can be obtained. Furthermore, it is expected that the identified transitions match the known locations of the inflection point, maximum, and zero-crossing.

The B&B was run first using both possible cases of shape verification (See Section 2.3.4; case 1 and 2). With this approach, the optimal solution was found with verification in 19 branching steps (38 nodes, 78 SOCPs). When applying only the known case for shape verification (See Section 2.3.4; case 1) the same solution was found in 142 branching steps (288 nodes, 570 SOCPs).

Fig. 6 displays the obtained results. The top panel shows the sampled data points, the knots of the sampled function (True knots), and the true transitions as well as the optimized SCS function and the location of the optimized transitions. One cannot visually distinguish between the locations of the true and optimized transitions. The differences between the true values and the obtained values are 1.99×10^{-4}, 4.11×10^{-7} and 3.73×10^{-8} respectively. As such, the obtained values for the transitions are the true values (1.20, 1.69, and 2.28) within excellent precision. The bottom panel of Fig. 6 displays the prediction residual for the fitted function, i.e., the difference between the fitted function and the true function. The absolute value of these prediction residuals is smaller than 3×10^{-5} over the whole domain of the true function. As such, the B&B algorithm results in retrieving the original, true function within acceptable precision.

3.3. Case study: Diagnosis of a fed-batch reactor

To demonstrate the potential of the developed method, the following paragraphs present a case study in which the generalized SCS function fitting method is used for fault diagnosis of a fed-batch batch reactor. The case study is explained first (Section 3.3.1). Then, the applied diagnostic procedures are presented (Section 3.3.2). Diagnostic results are presented in Section 3.3.3 and computational demand of the evaluated procedures are given in Section 3.3.4.

3.3.1. Case study

In Monroy, Villez, Graells, and Venkatasubramanian (2011), the simulation model of Birol, Undey, and Ç inar (2002) is simulated under various normal and abnormal conditions to test fault diagnosis methods based on quantitative models, including Principal Component Analysis (PCA) and Independent Component Analysis (ICA) as models for data dimension reduction and Artificial Neural Networks (ANNs) and Support Vector Machines (SVMs) as classification models. In Villez et al. (2012) the same data was used for benchmarking of a tool for qualitative representation of trends based on wavelets (Bakshi & Stephanopoulos, 1994). In the current study, 30 batches are simulated and analyzed with the purpose of assessing diagnostic performance of the newly proposed method. The first 10 batches correspond to normal operational conditions (NOC). Batch 11–20 are simulated with a reduced saturation constant (K_x) from 0.15 g/l (nominal value) to values ranging between 0.3 and 0.9 g/l (Fault 1). Batch 21–30 are simulated with a reduction of the substrate feed rate in the fed-batch stage to values ranging from 0.001 to 0.01 l/h (Fault 2). Each batch lasts 400 h. The analyzed data consists of the Penicillin concentration measurement

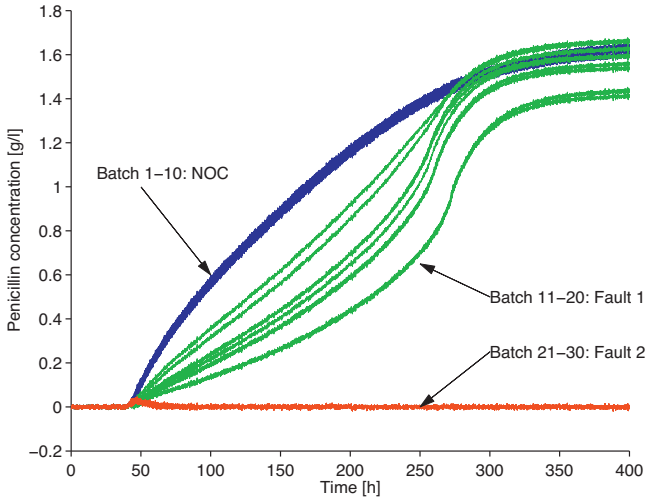

Fig. 7. Penicillin concentration profiles for different process conditions. The qualitative representation based on visual inspection is unique for each process condition.

series obtained in each batch. The noise-free simulations of these concentration profiles are used to determine the true location of extrema and inflection points by simple differentiation. The noise-free concentration values are obtained by sampling the simulated concentration at every 0.04 h (4.80 min). Noisy measurements are obtained by adding 25 white noise sequences (Gaussian distribution) with four (4) different standard deviations ($\sigma \in \{.0032, 0.01, 0.032, 0.1\}$) to each batch profile. This leads to the analysis of 3750 ($=30 \cdot 25 \cdot 5$) time series, including the noise-free time series. For more details on the simulated data we refer to Monroy et al. (2011) and Villez et al. (2012).

Concentration measurement series for the 30 simulated batches are plotted in Fig. 7 for $\sigma = 1e-2$ with the same, 1st, noise sequence. At this noise level, the signal to noise ratio (SNR, standard deviation of noisy measurements to standard deviation of noise) is 63.2 for all batches. The SNR values for batches under the NOC, Fault 1, and Fault 2 scenarios are 55.6, 58.9, and 0.466. By visual inspection, batches 1–10, 11–20 and 21–30 are recognized to be of BC, BCBC, and BCDA shape, respectively.

The former visual assessment suggests that qualitative representations of trends can be used to discriminate between different batch conditions. This was tested with limited success based on the wavelet-based method in Villez et al. (2012). Here, we do the same while using the newly developed method to obtain optimal QRs and compare with the method of Villez et al. (2012). Provided such discrimination can be executed successfully and timely, supervisory control can be automated so to mitigate consequences of faulty conditions in a given batch and restore normal operation in subsequent batches.

One may observe that each batch starts with a flat episode (F) and that the batches corresponding to Fault 2 end with an approximately flat episode. While this is correct, it leads to the requirement to optimize the location of additional endpoints of such an F episode, leading to higher computational demand. For this reason, such equality-constrained shapes are ignored for this case study. It is also noted that the B and A shapes are defined by a non-strict inequalities (lower or equal to, higher or equal to) which permits zero-valued derivatives.

3.3.2. Diagnostic procedure

To enable diagnosis on the basis of qualitative analysis of trends, a qualitative sequence (QS) is matched with each possible process condition. Each QS can be reduced to a monotonic sequence by only considering the first-order derivatives. In addition, the presented

Table 2
Process conditions, qualitative sequences (QSs), and prior likelihoods.

Condition	Qualitative sequence (QS)	Monotonic	Prior likelihood
Normal Operation Conditions (NOC)	BC	U	1.00
Fault 1	BCBC	U	0.99
Fault 2	BCDA (=BNA)	UL	0.99

diagnostic procedures (see below) require a prior likelihood associated with each condition. Triplets of process conditions, QSs, and prior likelihoods are listed in Table 2 for this study. One can see, that a slightly higher prior likelihood is given to NOC (BC). This is done so because the BCBC and the BCDA sequences leave more degrees freedom than the BC sequence and potentially deliver a better fit and thus higher likelihood. The applied prior likelihoods assist in offsetting this advantage and have been set by trial and error due to lack of a formal method to define priors on QSs. This challenge is discussed further in Section 4. Note that the BCDA sequence is the same as a BNA sequence as the two inflection points in a BNA sequence imply a maximum in between them, as is also discussed in Section 3.

The diagnosis task can then be executed as follows:

1 For each possible condition and associated QS, optimize the location of extrema and inflection points implied in the QS with the presented B&B algorithm. The negative log-likelihood of the data conditional to the QS is used as the objective function to be minimized.
2 After optimization, compute the likelihood of the data conditional to the computed QR for each of the possible conditions. This is the maximum likelihood conditional to each QS.
3 Multiply the maximum likelihoods as computed in step 2 with the prior likelihood for each condition. Normalize these likelihoods so they sum to one. This results in the MAP probability for each QS.
4 Select the QS and associate condition with maximum value for the computed MAP.

The above procedure is applied for 30 batches used in this study, particularly those with $\sigma = 0.01$ and with the same first noise sequence. In what follows, we refer to this procedure as the Shape Constrained Spline Diagnosis Procedure 1 (SCSDP1). The negative log-likelihood in step 1 is the exponential of the sum of squared residuals (SSR):

$$-\log(L(y,c)) = J(y,c) = \sum_{j=1}^{n}(y_j - f(x_j,\mathbf{c}))^2 = SSR \tag{39}$$

This is a convex function of the spline coefficients. As such the SOCP and B&B methods remain valid. The spline knots are placed at every 50th measurement, leading to 101 spline coefficients for each time series.

To investigate potential improvements in computational demand, a slightly different diagnostic procedure was tested as an alternative on all the batches. The steps are as follows and are specific to this case study.

1 Compute the location of inflection points implied in the sequence BNA (corresponding to Fault 2) with the presented B&B algorithm. The same objective function is used. The MAP for the sequence BNA is computed and referred to as L_{BNA}.
2 Compute the SCS function with a single monotonic sequence, U (upward trend). Since no extrema or inflection points are to be located, this can be solved as a single SOCP. Compute the associated maximum posterior likelihood by multiplying the data likelihood with 1.01 and refer to this likelihood as L_U.
3 If $L_U < L_{BNA}$, then the diagnosis result is that BNA, and thus Fault 2, is most likely. This ends the diagnosis procedure. Otherwise, go to step 4.
4 If $L_U > L_{BNA}$, then continue computations so to compute the maximum posterior likelihood conditional to the remaining QSs (L_{BC}, L_{BCBC}). Normalize the resulting likelihoods and select the condition which has maximum posterior probability. I.e., MAP probability is used to select the final diagnosis result.

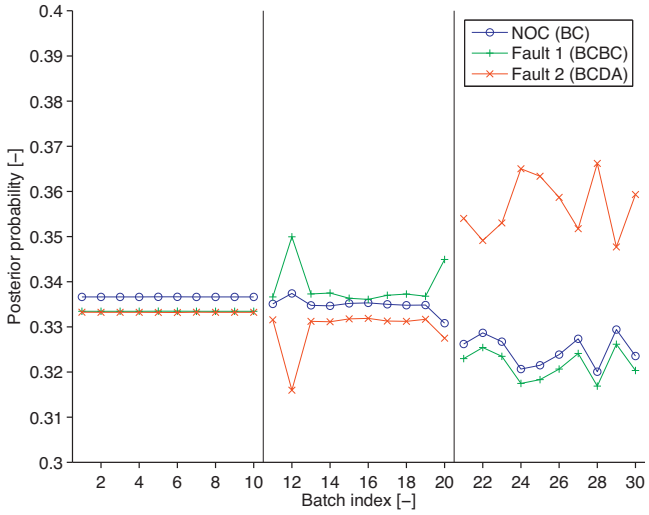

Fig. 8. The Maximum A Posteriori (MAP) probability obtained with the Shape Constrained Spline Diagnosis Procedure 1 (SCSDP1) as a function of batch index.

This second procedure is referred to as Shape Constrained Spline Diagnosis Procedure 2 (SCSDP2). This procedure is guaranteed to deliver the same diagnostic result as the SCSDP1 because L_U is an upper bound for the MAP for both the BC and BCBC sequences. This is true because the BC and BCBC include all monotonicity constraints associated with the U sequence as well as additional constraints on the second derivative. For this reason, the negative log-likelihood for the optimal BC and BCBC representations cannot be lower than the negative log-likelihood for the U sequence. Furthermore, if $L_{BNA} > L_U$, one is sure that the L_{BC} and L_{BCBC} values cannot be higher than L_U and one can select the BNA sequence as most likely without computing the optimal location of the inflection points in the BC and BCBC sequences. The SCSDP2 is thus potentially computationally beneficial without losses in accuracy.

The results obtained with the wavelet-based method for qualitative analysis as used in Villez et al. (2012) for the same batches are used here for comparison. This comparison includes (1) the accuracy of diagnosis and (2) computational requirements for each method.

3.3.3. Diagnostic results

Detailed results are first presented for 30 simulated batches only, namely for the 30 simulated batches with $\sigma = 0.01$ and applying the same first noise sequence. The posterior probabilities as computed with the SCSDP1 are shown in Fig. 8. It can be seen that maximum values for the MAP likelihood are obtained for the true QS. Still, the MAP values are fairly close to each other, especially for the NOC and Fault 1 batches, possibly suggesting that the method may not be very robust. With the SCSDP2, the results (not shown) differ only for batch 21–30. Here, only the inflection points in the BNA representation are optimized for batches 21–30 as the likelihood for the upward. Thus, with the SCSDP2 it is only known that

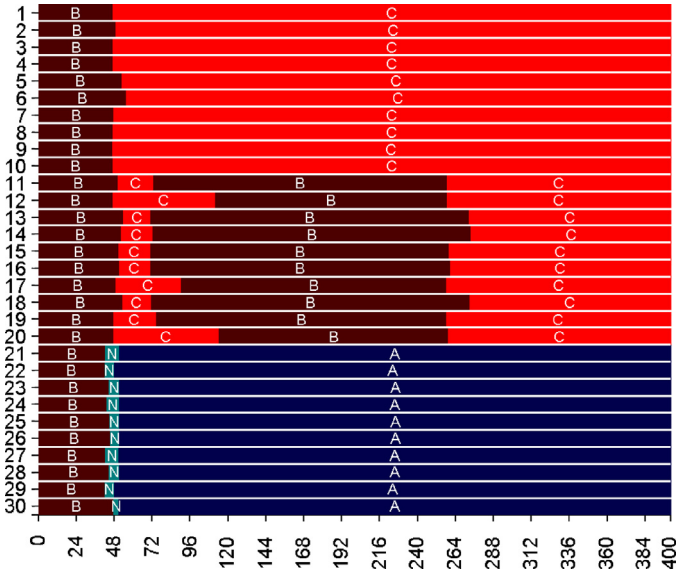

Fig. 9. Qualitative representations (QRs) obtained with the Shape Constrained Spline (SCS) diagnosis method. Each horizontal bar represents one batch. Red is used for upward trends and blue for downward trends. Darker tones correspond to convex curvature, light tones to concave curvature. (For interpretation of the references to color in this figure legend, the reader is referred to the web version of the article.)

the MAP for the BNA sequence is higher than the MAPs for the BC and BCBC sequences. This is sufficient for diagnosis.

The QRs corresponding to the maximum MAP value for the 30 selected batches (batches with $\sigma = 0.01$ and first noise sequence) are displayed in Fig. 9. As observed before, the SCS method obtains perfect classification as the displayed sequences are the correct ones.

To investigate why the MAP values for different sequences can be so close, as shown in Fig. 8, Fig. 10 shows all the obtained QRs corresponding to the first ten batches. Thus, for each of these ten batches, three QRs, corresponding to the BC, BCBC, and BNA sequences, are displayed. Interestingly, two of the three inflection

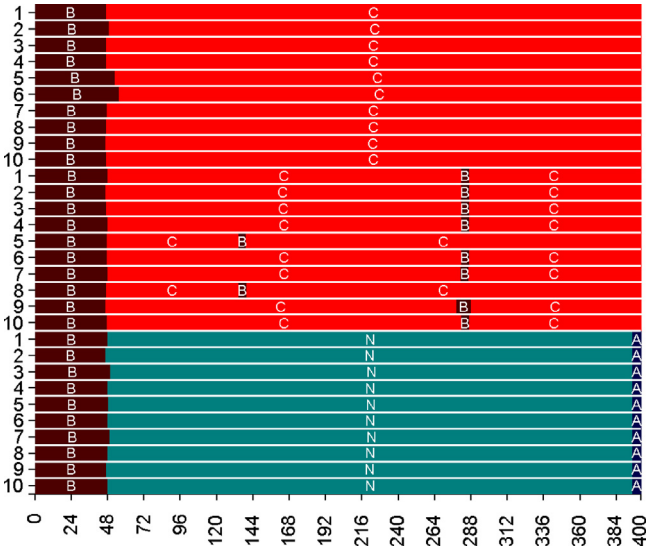

Fig. 10. Qualitative representations (QRs) obtained with the Shape Constrained Spline (SCS) diagnosis method for batches 1–10. Each horizontal bar represents one batch. Red is used for upward trends, blue for downward trends and green for the concave episode. The bars are displayed in groups of 10 corresponding to the BC, BCBC, and BNA sequences (top to bottom). (For interpretation of the references to color in this figure legend, the reader is referred to the web version of the article.)

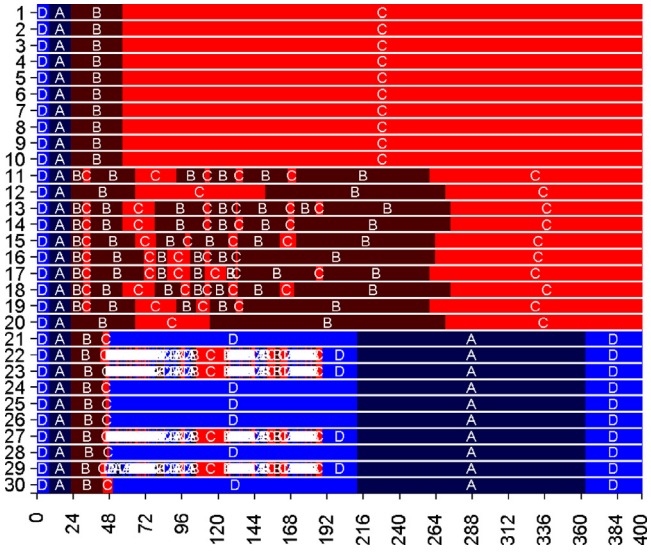

Fig. 11. Qualitative representations (QRs) obtained with the wavelet-based method.

points in the BCBC representation are always close to each other and the last inflection point in the BNA sequence is always very near to the end of the batch length. It was further visually confirmed that the implied maximum in the BNA representations is also close to the end of the batch. This is an indication of why the MAP values can be so close. Indeed, the added primitives in the BCBC and BNA sequences, compared to the BC sequence, have limited effects on the obtained SSR, and thus the MAP, because the identified episodes are rendered small by means of the optimization method. In the discussion section, the possible negative effects of this and possible ways to circumvent it are discussed.

The QRs obtained by the wavelet-based method are shown in Fig. 11. Here one sees that no single QR is identified correctly, which is a further indication of this method's extreme sensitivity to moderate levels of noise as reported in Villez et al. (2012).

From here on, diagnostic results obtained with results for the whole simulation study (all noise levels and noise sequences) are discussed. In Fig. 12, the fraction of correctly classified batches

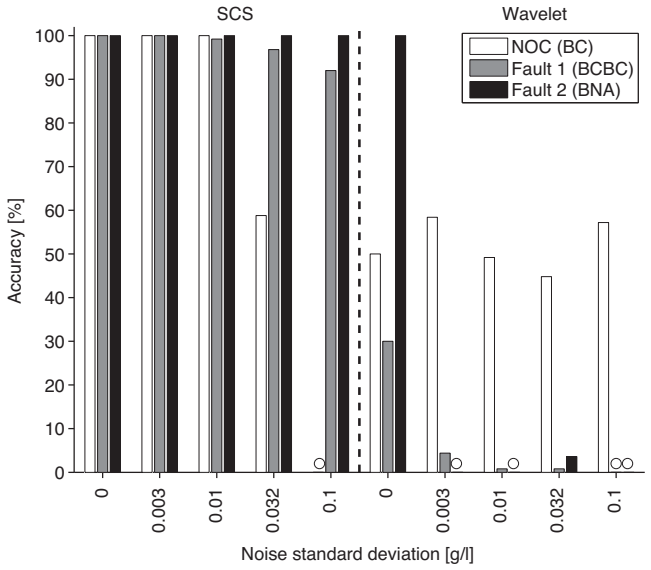

Fig. 12. Accuracy of the fault diagnosis procedure with the SCS method (left) and the wavelet-based method (right) as function of the noise standard deviation and process condition. Circles indicate zero accuracy.

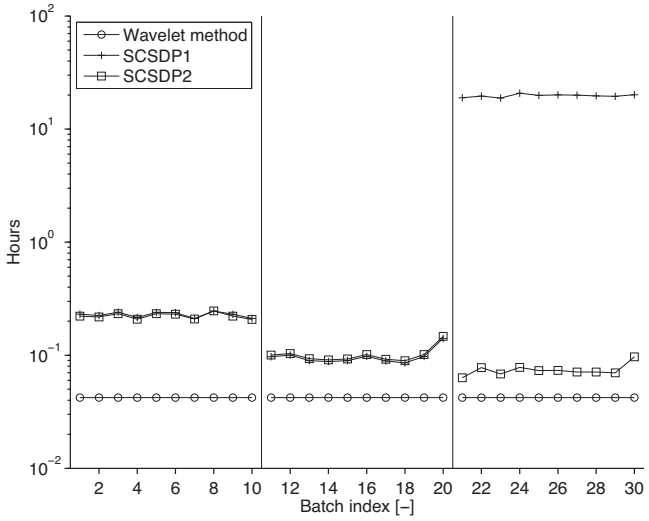

Fig. 13. Computational time needed for diagnosis of 30 selected batches.

(accuracy) is displayed for each noise level and for each process condition. Each fraction is thus based on 250 batches (10 simulated batches with 25 noise sequences). It can be seen that the SCS method outperforms the wavelet-based method by large margins except for NOC batches at the highest noise level. The reason for this is that the wavelet-based method classifies a large fraction of the batches as unknown. This is because the resulting QR does not match any of the previously identified QSs (BC, BCBC, BCDA). This was also be observed in Fig. 9. Increasing the noise level reduces the accuracy of the SCS method. The accuracy remains above 90% however for batches with fault 1 and 2, even at the highest noise level. For NOC batches, it reduces to zero at the highest level. This is because a large fraction of the NOC batches is classified as a fault 2 batch. In supplementary materials, one can find frequency tables for both the SCS and wavelet-based method which further demonstrate the dramatic increase in performance with the proposed method.

3.3.4. Computational demand

The B&B algorithm is renown for its high computational demand. As such, checking the time needed for a diagnostic result should not be ignored in the evaluation of the new method. Fig. 13 shows the time needed for the diagnosis task with the newly developed method (SCSDP1 and SCSDP2) as well as with the method of Villez et al. (2012) on the same PC (Pentium IV, 3 GHz, 1,GB RAM). The results shown are for the same 30 batches as discussed above ($\sigma = 1e-2$ with the same, 1st, noise sequence). Several conclusions can be drawn regarding the computational time demand. First, the time needed for the original wavelet-based method is nearly constant and amounts to 2.5 min (0.04 h). In contrast, the method based on SCS function fitting has a widely varying time demand ranging from about 5 min (0.08 h) for batches 11–20 up to 20 h for batches 21–30. Because the computational demand is fairly constant for each group of batches (1–10, 11–20, 21–30), it is clear that the computational time is highly sensitive to the true shape of the analyzed time series. This is not so with the original method of Villez et al. (2012).

The SCSDP1 and SCSDP2 need about the same computational time for batches 1–20. In contrast, for batches 21–30, the SCSDP2 procedure requires less than 6 min while the SCSDP1 more than 18 h for these batches. This discrepancy is due to the fact that with the SCSDP2 procedure the B&B algorithm was only used once for the computation of extremum and inflection points in the BCDA representation. Each time, the resulting posterior likelihood for this

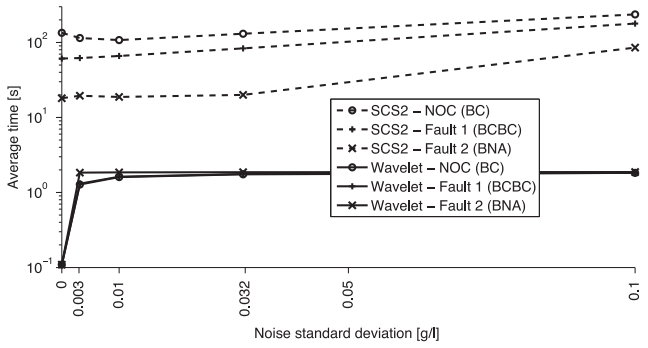

Fig. 14. Average computational time needed for diagnosis of all batches.

sequence (L_{BCDA}) was higher than the likelihood for the U sequence (L_U) so that the optimization for the BC and BCBC sequence is not executed.

The effect of noise on the computational requirements for the SCS method is only studied with SCSDP2, because of the high computational demand associated with the SCSDP1. The average times needed to obtain the diagnostic result, each based on 250 batches, are plotted in Fig. 14 as function of the standard deviation. As observed above, the required time is up to a factor 100 larger for the SCS method (SCSDP2) compared to the wavelet based method. Also, the computational time is influenced by the simulated fault scenario, with decreasing requirements for NOC, Fault 1, and Fault 2 conditions. One can see that increasing noise levels increase the computational demand for the SCSDP2, though this is not a dramatic effect. The wavelet method is generally unaffected by the noise level, except that the complete absence of noise reduces the computational requirements by a factor 10.

4. Discussion

Generalization of univariate Shape Constrained Spline (SCS) function fitting

With this manuscript a globally optimal method for univariate SCS function fitting is presented. The optimal argument values for changes between primitives in a qualitative sequence (QS) can be found with a branch and bound (B&B) algorithm. The lower and upper bounds which are necessary for its validity were provided with detailed proofs based on a Second Order Cone Program (SOCP) formulation of SCS function fitting.

Global optimality for data mining

Historical developments in the context of qualitative analysis are characterized by ample use of heuristics and are therefore often suboptimal in a statistical sense. The provided method is optimal in the maximum likelihood sense. In addition, the use of a deterministic global optimization approach is rather unique in the context of

nonlinear data mining methods. It is more typical to use local optimization methods such as the EM algorithm or stochastic optimization methods such as genetic algorithms. Exceptions are found in the context of Feed-Forward Neural Networks (Tang & Koehler, 1994; Toh, 2003).

Discriminative power It was observed in the fault diagnosis case study that dissimilar QSs can still lead to very similar values for the likelihood. One important aspect is that the method as applied does not limit or guarantee the distance between any two consecutive endpoints. The result is that consecutive episode endpoints can be very close to each other, thereby reducing the impact of the presence of a particular primitive within a QS on the overall function fit. This reduces the discriminative power of the method, which is however successfully accounted for in this study by a prior likelihood for each QS. To improve this power, one may implement a minimal distance constraint on the episode endpoints. This would imply a uniform prior over the set of feasible episode endpoints. Practically, it would imply a rather simple adjustment of the QP used to identify a feasible point. Similarly, Dash et al. (2004) provide a threshold on the length of any episode. Alternatively, the proposed method allows also to use a smooth prior on the episode endpoints, e.g., by including a penalty term on the episode endpoint distances. Both modifications however require adjustment of the bounding procedures and also introduces additional meta-parameters (minimal distance parameter or penalty parameter) which require additional tuning of method.

Limitations The provided method has some limitations in its current form. These include that (1) the method does not handle multivariate data series and (2) does not permit multiple independent variables, e.g., for shape constrained estimation of surfaces. In addition, (3) the fitted spline function cannot have discontinuities (knots with multiplicity), in turn implying that (4) certain QSs are not permitted. Furthermore, (5) it is assumed that one or more plausible QSs are given and (6) that the associated prior likelihoods for the QSs can be identified based on expert knowledge, neither if which is necessarily true. Finally, (7) no efficient method is yet available to compute confidence bounds on the spline coefficients or fitted function. Of limited concern is that there is a maximum for the allowed number of episode endpoints can be located between two knots of a spline. As indicated in the text, this is accommodated easily by adding additional knots.

Current and future research efforts are aimed at eliminating the above limitations. For example, an extension for multivariate time series (limitation 1) underwent preliminary tests already (Thuerlimann & Durrenmatt, 2013). Allowing for multiple inputs (limitation 2) is likely a hard problem. However, it also appears irrelevant for process diagnosis as time has been the only independent variable considered so far in the context of process diagnosis based on qualitative analysis. Still, Papp (2011) gives an overview of available approaches for multiple input variables. Preliminary results (unpublished) indicate that limitation 3 and 4 can be addressed by further relaxations of the SCS fitting problem, leading to more general yet more complex bounding procedures and slower convergence of the B&B algorithm. To address limitation 5, the QS itself needs to be included in the mathematical program. For limitation 6 and 7, Monte Carlo simulations are likely

a good yet lengthy solution to compute Bayes factors (limitation 6) and credible intervals (limitation 7). Approximate solutions may also be suitable, e.g., by making use of the Unscented Transform (Julier, 2002).

Computational time The B&B algorithm is known to be computationally intensive for problems with many parameters to be optimized. This was especially observed for the batch reactor case study. Given that one batch lasts about 400 h, 20 h of computation may be feasible for similar applications in industrial practice where off-line or end-of-batch assessment is warranted. However, the presented method may not be suitable for on-line application. In the particular study shown, a second procedure allowed a reduction of the computational time to less than 10 min for all considered batches. This second procedure took extra information about the considered QSs and their associated likelihoods into account. As it is not certain that such information is always available, such performance cannot always be expected. However, this result shows that a careful analysis of the considered QSs can assist in obtaining a reasonably fast diagnosis procedure without losing optimality.

It is also noted here that a very basic version of B&B algorithms is implemented with conventional rules for node selection and variable selection. Extended versions (e.g., branch-and-reduce, branch-and-cut) or other rules will be investigated as a means to reduce the computational time. Also, an initial guess of the episode endpoints can be used to provide a better upper bound at the root node. Such an initial guess could be obtained by means of faster but suboptimal methods for qualitative analysis by visual inspection. Naturally, such visual inspection would be time-consuming is and is likely prohibitive for large data bases. Alternative but suboptimal methods for qualitative trend analysis (Venkatasubramanian et al., 2003) may be easier to achieve initial guesses. A method which is expected to be particularly useful is presented in Villez and Rengaswamy (2013). It is based on solving an approximation of the SOCPs as solved in this work and allows to use more efficient algorithms such as Dynamic Programming (DP) (Keogh, 2002). Finally, different formulations of the problem as already explored in Papp (2011) may studied further to obtain faster solution schemes.

Applications The presented method for generalized SCS function fitting is expected to be broadly applicable. In this study, we demonstrated its application for batch process diagnosis. In the future, we expect to evaluate the method in the context of data reconciliation, data clustering and, classification. Solving such problems may further lend itself to improved fault detection and diagnosis and pattern discovery and recognition in dynamic processes. An important advantage of qualitative analysis in this context over other, quantitative, data mining methods is the amount of data needed for proper tuning of the presented method is very limited.

5. Conclusions

With this manuscript a generalized method for univariate Shape Constrained Spline (SCS) function fitting is provided and demonstrated. The method builds further on earlier work in which SCS function fitting was recognized to be equivalent to solving a Second Order Cone Program (SOCP). The proposed method extends the existing approach by searching proper identification of the so called episode endpoints which can signify zero crossings, extrema, and inflection points. This identification is globally optimal thanks to the use of the branch-and-bound (B&B) algorithm. The lower and upper bounds which are prerequisites for application of this algorithm were explained in detail and proven valid.

In addition to the generalization of existing SCS-based methods, some barriers in the context of qualitative analysis have been removed. First of all, the method is globally optimal in a maximum likelihood sense, which is a first in this research area. Second, the method only needs a qualitative sequence (QS) as a shape

constraint, i.e., a sequence of sets of signs for the fitted function and its derivatives. Such sequences are often provided by process experts as target patterns without specifying the transition times between the sets of signs. As such, the method allows optimal recognition of such target patterns, as was demonstrated. Furthermore, the QS which functions as a shape constraint for spline fitting is also of the same format of qualitative simulation results. Because of this, it is expected that SCS function fitting can be used to compare and select different qualitative models based on experimental data.

The global optimality of the method means that the method can be used for benchmarking of other, faster methods for on-line applications. Unfortunately, the provided method is considered too slow for real-time on-line applications. Therefore, future work will focus on the development of methods which are substantially faster while closely approximating the optimality of the provided method.

Acknowledgements

We want to thank Mr. Papp for his assistance in interpreting his work in Papp (2011). All results were obtained by joint use of Matlab (The MathWorks Inc., 2010); the Functional Data Analysis software package accompanying the book (Ramsay & Silverman, 2002); and MOSEK (Andersen & Andersen, 2000; MOSEK ApS, 2012).

Appendix A. Supplementary data

Supplementary data associated with this article can be found, in the online version, at http://dx.doi.org/10.1016/j.compchemeng.2013.06.005.

References

Alizadeh, F., & Goldfarb, D. (2003). Second-order cone programming. *Mathematical Programming, Series B*, *95*, 3–51.
Andersen, E. D., & Andersen, K. D. (2000). The MOSEK interior point optimizer for linear programming: An implementation of the homogeneous algorithm. *High Performance Optimization*, *33*, 197–232.
Bakshi, B. R., & Stephanopoulos, G. (1994). Representation of process trends – Part III, Multiscale extraction of trends from process data. *Computers and Chemical Engineering*, *18*, 267–302.
Beliakov, G. (2000). Shape preserving approximation using least squares splines. *Analysis in Theory and Applications*, *16*, 80–98.
Birol, G., Undey, C., & Ç inar, A. (2002). A modular simulation package for fed-batch fermentation: Penicillin production. *Computers and Chemical Engineering*, *26*, 1553–1565.
de Boor, C. (1978). *A practical guide to splines*. New York: Springer-Verlag.
Brunk, H. D. (1955). Maximum likelihood estimates of monotone parameters. *Annals of Mathematical Statistics*, *26*, 607–616.
Bryman, A., & Burgess, R. (1993). *Analysing qualitative data*. New York, NY: Routledge.
Cai, B., & Dunson, D. B. (2007). Bayesian multivariate isotonic regression splines: Applications to carcinogenicity studies. *Journal of the American Statistical Association*, *102*, 1158–1171.
Cao, S., & Rhinehart, R. R. (1995). An efficient method for on-line identification of steady state. *Journal of Process Control*, *5*, 363–374.
Charbonnier, S., Garcia-Beltan, C., Cadet, C., & Gentil, S. (2005). Trends extraction and analysis for complex system monitoring and decision support. *Engineering Applications of Artificial Intelligence*, *18*, 21–36.
Cheung, J.-Y., & Stephanopoulos, G. (1990). Representation of process trends – Part I. A formal representation framework. *Computers and Chemical Engineering*, *14*, 495–510.
Colomer, J., Melendez, J., & Gamero, F. (2002). Qualitative representation of process trends for situation assessment based on cases. In *IFAC World Congress 2002, Barcelona, Spain*
Cox, M. G., Harris, P. M., & Jones, H. M. (1990). A knot placement strategy for least squares spline fitting based on the use of local polynomial approximations. *Algorithms for Approximation II*, 37–45.
Dash, S., Maurya, M. R., Venkatasubramanian, V., & Rengaswamy, R. (2004). A novel interval-halving framework for automated identification of process trends. *AIChE Journal*, *50*, 149–162.
Delecroix, M., Simioni, M., & Thomas-Agnan, C. (1996). Functional estimation under shape constraints. *Journal of Nonparametric Statistics*, *6*, 69–89.
Delecroix, M., & Thomas-Agnan, C. (2000). Spline and kernel smoothing under shape restrictions. In M. Schimek (Ed.), *Smoothing and regression: approaches, computation and application* (pp. 109–134). New York: Wiley.
Dette, H., Neumeyer, N., & Pilz, K. F. (2006). A simple nonparametric estimator of a strictly monotone regression function. *Bernoulli*, *12*, 469–490.
Dette, H., & Pilz, K. F. (2006). A comparative study of monotone nonparametric kernel estimates. *Journal of Statistical Computation and Simulation*, *76*, 41–56.
Dierckx, P. (1980). An algorithm for cubic spline fitting with convexity constraints. *Computing*, *24*, 349–371.
Dykstra, R. L. (1983). An algorithm for restricted least squares regression. *Journal of the American Statistical Association*, *78*, 837–842.
Elfving, T., & Andersson, L.-E. (1988). An algorithm for computing constrained smoothing spline functions. *Numerische Mathematik*, *52*, 583–595.
Flehmig, F., & Marquardt, W. (2006). Detection of multivariable trends in measured process quantities. *Journal of Process Control*, *16*, 947–957.
Flehmig, F., Watzdorf, R., & Marquardt, W. (1998). Identification of trends in process measurements using the wavelet transform. *Computers and Chemical Engineering*, *22*, S491–S496.
Floudas, C. A., & Gounaris, C. E. (2009). A review of recent advances in global optimization. *Journal of Global Optimization*, *45*, 3–38.
Forst, W., & Hoffmann, D. (2010). *Optimization – Theory and practice*. New York: Springer.
Fraser, D. A. S., & Massam, H. (1989). A mixed primal-dual bases algorithm for regression under inequality constraints, application to concave regression. *Scandinavian Journal of Statistics*, *16*, 65–74.
Friedman, J., & Tibshirani, R. (1984). The monotone smoothing of scatterplots. *Technometrics*, *26*, 243–250.
Friedman, J. H. (1991). Multivariate adaptive regression splines. *The Annals of Statistics*, *19*, 1–67.
Fritsch, F. N. (1990). *Algorithms for approximation II. Chapter Monotone piecewise cubic data fitting*. London: Chapman and Hall.
Grant, M., & Boyd, S. (2011). *CVX: Matlab software for disciplined convex programming, version 1.21*. Available from http://cvxr.com/cvx
Habtzghi, D., & Datta, S. (2012). One sample goodness of fit tests in presence of shape restrictions on the hazard rate function. *Sankhya B - Applied and Interdisciplinary Statistics*, *74*, 171–194.
Hall, P., Huang, L.-S., Gifford, J. A., & Gijbels, I. (2001). Nonparametric estimation of hazard rate under the constraint of monotonicity. *Journal of Computational and Graphical Statistics*, *10*, 592–614.
Hastie, T., Tibshirani, R., & Friedman, J. (2001). *The elements of statistical learning. Data mining, inference, and prediction*. NY, USA: Springer.
Hazelton, M. L., & Turlach, B. A. (2011). Semiparametric regression with shape constrained penalized splines. *Computational Statistics and Data Analysis*, *55*, 2871–2879.
He, X., & Shi, P. (1998). Monotone B-spline smoothing. *Journal of the American Statistical Association*, *93*, 643–650.
Holmes, C. C., & Heard, N. A. (2003). Generalized monotonic regression using random change points. *Statistics in Medicine*, *22*, 623–638.
Hölzle, G. E. (1983). Knot placement for piecewise polynomial approximation of curves. *Computer-Aided Design*, *15*, 295–296.
Janusz, M. E., & Venkatasubramanian, V. (1991). Automatic generation of qualitative description of process trends for fault detection and diagnosis. *Engineering Applications of Artificial Intelligence*, *4*, 329–339.
Julier, S. J. (2002). The scaled unscented transformation. In *Proceedings of the American control conference, Anchorage, AK, May 8–10, 2002* (pp. 4555–4559).
Jupp, D. L. B. (1978). Approximation to data by splines with free knots. *SIAM Journal on Numerical Analysis*, *15*, 328–343.
Kelly, C., & Rice, J. (1990). Monotone smoothing with application to dose-response curves and the assessment of synergism. *Biometrics*, *46*, 1071–1085.
Keogh, E. (2002). Exact indexing of dynamic time warping. In *Proceedings of the 28th international conference on very large data bases 2002 (VLDB2002)* (pp. 406–417).
Kuipers, B. J. (1994). *Qualitative reasoning: Modeling and simulation with incomplete knowledge*. Cambridge, MA: MIT Press.
Lavine, M., & Mockus, A. (1995). A nonparametric Bayes method for isotonic regression. *Journal of Statistical Planning and Inference*, *46*, 235–248.
Lawler, E. L., & Wood, D. E. (1966). Branch-and-bound methods: A survey. *Operations Research*, *14*, 699–719.
Leitenstorfer, F., & Tutz, G. (2007). Generalized monotonic regression based on B-splines with an application to air pollution data. *Biostatistics*, *8*, 654–673.
MacKay, D. (2003). *Information theory, inference, and learning algorithms*. Cambridge: Cambridge University Press.
Mammen, E. (1991). Estimating a smooth monotone regression function. *The Annals of Statistics*, *19*, 724–740.
Mammen, E., Marron, J. S., Turlach, B. A., & Wand, M. P. (2001). A general projection framework for constrained smoothing. *Statistical Science*, *16*, 232–248.
Mammen, E., & Thomas-Agnan, T. (1999). Smoothing splines and shape restrictions. *Scandinavian Journal of Statistics*, *26*, 239–252.
Maurya, M. R., Paritosh, P. K., Rengaswamy, R., & Venkatasubramanian, V. (2010). A framework for on-line trend extraction and fault diagnosis. *Engineering Applications of Artificial Intelligence*, *23*, 950–960.
Maurya, M. R., Rengaswamy, R., & Venkatasubramanian, V. (2005). Fault diagnosis by qualitative trend analysis of the principal components. *Computers and Chemical Engineering*, *83*, 1122–1132.

Meyer, M. C. (1999). An extension of the mixed primal-dual bases algorithm to the case of more constraints than dimensions. *Journal of Statistical Planning and Inference*, *81*, 13–31.
Meyer, M. C. (2008). Inference using shape-restricted regression splines. *Annals of Applied Statistics*, *2*, 1013–1033.
Meyer, M. C., & Habtzghi, D. (2011). Nonparametric estimation of density and hazard rate functions with shape restrictions. *Journal of Nonparametric Statistics*, *23*, 455–470.
Miles, M., & Huberman, A. (Eds.). (1994). *Qualitative data analysis: An expanded sourcebook*. Thousand Oaks, CA: Sage.
Mitten, L. G. (1970). Branch-and-bound methods: General formulation and properties. *Operations Research*, *18*, 24–34.
Monroy, I., Villez, K., Graells, M., & Venkatasubramanian, V. (2011). Fault diagnosis of a benchmark fermentation process: A comparative study of feature extraction and classification techniques. *Bioprocess and Biosystems Engineering*, *35*, 689–704. http://dx.doi.org/10.1007/s00449-011-0649-1
MOSEK ApS. (2012). *MOSEK optimization software for MATLAB, version 6.0*. Available from http://www.mosek.com/
Mukerjee, H. (1988). Monotone nonparametric regression. *Annals of Statistics*, *16*, 741–750.
Nesterov, Y. (2000). . *High performance optimization, applied optimization. Chapter Squared functional systems and optimization problems* (vol. 33) Kluwer Academic Publishers.
Papp, D. (2011). *Optimization models for shape-constrained function estimation problems involving nonnegative polynomials and their restrictions* (Ph.D. thesis). Rutgers University.
Parker, R. G., & Rardin, R. L. (1988). *Discrete optimization*. New York, NY: Academic Press.
Ramsay, J. O. (1988). Monotone regression splines in action. *Statistical Science*, *3*, 425–441.
Ramsay, J. O. (1998). Estimating smooth monotone functions. *Journal of the Royal Statistical Society, Series B*, *60*, 365–375.
Ramsay, J. O., & Silverman, B. W. (2002). *Applied functional data analysis: Methods and case studies*. New York, NY: Springer-Verlag.
Ramsay, J. O., & Silverman, B. W. (2005). *Functional data analysis*. New York, USA: Springer.
Rengaswamy, R., & Venkatasubramanian, V. (1995). A syntactic pattern-recognition approach for process monitoring and fault diagnosis. *Engineering Applications of Artificial Intelligence*, *8*, 35–51.
Robertson, T., Wright, F. T., & Dykstra, R. L. (1988). *Order restricted statistical inference*. New York, NY: Wiley.
Rubio, M. J. C., Ruiz, M. L. J. C., & Mélendez, J. (2004). Qualitative trends for situations assessment in SBR wastewater treatment process. In *Proceedings of the 4th ECAI workshop on binding environmental sciences and artificial intelligence (BESAI)* August 2004, Valencia, Spain.
Stephanopoulos, G., Locher, G., Duff, M., Kamimura, R., & Stephanopoulos, G. (1997). Fermentation database mining by pattern recognition. *Biotechnology and Bioengineering*, *53*, 443–452.
Tang, Z., & Koehler, G. J. (1994). Deterministic global optimal FNN training algorithms. *Neural Networks*, *7*, 301–311.
Tantiyaswasdikul, C., & Woodroofe, M. B. (1994). Isotonic smoothing splines under sequential designs. *Journal of Statistical Planning and Inference*, *38*, 75–88.
The MathWorks Inc. (2010). *Matlab, version 7.10 0 (R2010a)*. Massachusetts: Natick.
Thuerlimann, C. M., & Durrenmatt, D. J. (2013). Qualitative trend analysis with shape constrained splines: Multivariate extension and validation with full-scale data. In *2013 AIChE annual meeting* San Francisco, November 3–8, (submitted for publication).
Toh, K.-A. (2003). Deterministic global optimization for FNN training. *IEEE Transactions on Systems, Man, and Cybernetics, Part B: Cybernetics*, *33*, 977–983.
Turlach, B. A. (2005). Shape constrained smoothing using smoothing splines. *Computational Statistics*, *20*, 81–103.
Utreras, F. I. (1985). Smoothing noisy data under monotonicity constraints: Existence, characterization, and convergence rates. *Numerische Mathematik*, *47*, 611–625.
Vapnik, V. (1995). *The nature of statistical learning theory*. New York, NY: Springer-Verlag.
Venkatasubramanian, V., Rengaswamy, R., & Kavuri, S. N. (2003). A review of process fault detection and diagnosis – Part II: Qualitative models and search strategies. *Computers and Chemical Engineering*, *27*, 313–326.
Villalobos, M., & Wahba, G. (1987). Inequality-constrained multivariate smoothing splines with application to the estimation of posterior probabilities. *Journal of the American Statistical Association*, *82*, 239–248.
Villez, K. (2007). *Multivariate and qualitative data analysis for monitoring, diagnosis and control of sequencing batch reactors for wastewater treatment* (Ph.D. thesis). Ghent University, Ghent, Belgium.
Villez, K., Keser, B., & Rieger, L. (2009). Qualitative representation of trends (QRT) as a tool for automated data-driven diagnostics for on-line sensors. In *Proceedings of the 7th IFAC symposium on fault detection, supervision and safety of technical processes (SafeProcess2009), Barcelona, Spain, 30 June–3 July, 2009, appeared on CD-ROM*.
Villez, K., Pelletier, G., Rosén, C., Anctil, F., Duchesne, C., & Vanrolleghem, P. A. (2007). Comparison of two wavelet-based tools for data mining of urban water networks time series. *Water Science and Technology*, *56*(6), 57–64.
Villez, K., & Rengaswamy, R. (2013). A generative approach to qualitative trend analysis for batch process fault diagnosis. In *Proceedings of the European Control Conference 2013 (ECC13)* Zürich, (pp. 1958–1963).
Villez, K., Rosén, C., Anctil, F., Duchesne, C., & Vanrolleghem, P. A. (2008). Qualitative representation of trends: An alternative approach to process diagnosis and control. *Water Science and Technology*, *57*(10), 1525–1532.
Villez, K., Rosén, C., Anctil, F., Duchesne, C., & Vanrolleghem, P. A. (2012). Qualitative representation of trends (QRT): Extended method for identification of consecutive inflection points. *Computers and Chemical Engineering*, *48*, 187–199.
Wang, X., & Li, F. (2008). Isotonic smoothing spline regression. *Journal of Computational and Graphical Statistics*, *17*, 1–17.
Wegman, E. J., & Wright, I. W. (1983). Splines in statistics. *Journal of the American Statistical Association*, *78*, 351–365.
Witkin, A. P. (1983). Scale-space filtering. In *Proc. 8th Int. Joint Conf. Art. Intell.* Karlsruhe, Germany, (pp. 1019–1022).
Wright, I. W., & Wegman, E. J. (1980). Isotonic, convex and related splines. *The Annals of Statistics*, *8*, 1023–1035.